Přílohy:

1. Linhart O., Smolejová J., Červený V., Hraníček J., **Nováková E.**, Resslerová T., Rychlovský P.: Determination of As by UV-photochemical generation of its volatile species with AAS detection, Monatshefte für Chemie, 2016, Volume 147, Pages 1447−1454, 10.1007/s00706-016−1808-5, IF: 1,131

Příloha je podkladem pro kapitolu 4.6.

2. **E. Nováková**, O. Linhart, V. Červený, P. Rychlovský and J. Hraníček: Flow Injection Determination of Se in Dietary Supplements Using TiO_2 Mediated UV-photochemical Volatile Species Generation, Spectrochim. Acta B, 2017, Volume 134, Pages 98-104, doi:10.1016/j.sab.2017.06.007, IF: 3,241

Příloha je podkladem pro kapitolu 4.3.2.

3. **E. Nováková**, M. Rybínová, J. Hraníček, P. Rychlovský, V. Červený: Comparison of interference in selenium volatile species generation methods with QF-AAS detection, J. Anal. At. Spectrom., *v recenzním řízení*

Příloha je podkladem pro kapitolu 4.6.

Vydané přílohy jsou v práci uvedeny se svolením vydavatele.

Monatsh Chem
DOI 10.1007/s00706-016-1808-5

ORIGINAL PAPER

Determination of As by UV-photochemical generation of its volatile species with AAS detection

Ondřej Linhart[1] · Jana Smolejová[1] · Václav Červený[1] · Jakub Hraníček[1] · Eliška Nováková[1] · Tina Resslerová[1] · Petr Rychlovský[1]

Received: 30 January 2016 / Accepted: 20 June 2016

Abstract This work was focused on the development of an analytical method for determination of arsenic in liquid (aqueous solutions of arsenite) by UV-photochemical generation of its volatile compounds. The study contains the optimization, method characterisation and also a study of the influence of selected compounds on the signal measured. The method involves a combination of flow injection analysis, UV-photochemical generation of volatile compounds of arsenic in flow injection arrangement and atomic absorption spectrometry using an externally heated quartz tube atomizer. The attained absorbance was very low after the optimization. In the next step, the influence of selected compounds on UV-photochemical generation was investigated with the aim to find a suitable reaction modifier that would improve the sensitivity of arsenic determination. Bi(III) was found as the best reaction modifier not only for causing the increase of the signal of arsenic measured but also for its persisting effect. The activation with concentration of 10 mg dm^{-3} of Bi(III) increases the absorbance of arsenic approximately eleven times compared to signals without activation. Following method characteristics were achieved under the optimum experimental conditions: the limit of detection of 18 μg dm^{-3}, the repeatability of 4.5 % expressed as % RSD at 200 μg dm^{-3}, and linear dynamic range 60–500 μg dm^{-3} of arsenic.

✉ Ondřej Linhart
linharo2@natur.cuni.cz

[1] Department of Analytical Chemistry, Faculty of Science, Charles University in Prague, Albertov 6, 128 43 Prague, Czech Republic

Graphical abstract

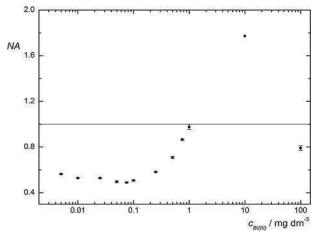

Keywords UV-photochemical generation · Arsenic · Photochemistry · Spectroscopy · Green chemistry · Ecology

Introduction

UV-photochemical generation of volatile compounds is important and well known technique in atomic spectrometry that can be used to determine metals, metalloids, or organometallic compounds. There are several approaches for conversion of the analyte from the aqueous phase into the gaseous phase. The chemical vapour generation (CVG) using borohydride as a reducing agent in the presence of mineral acid is the most popular way for the volatile compound forming elements. The common mixture is $NaBH_4$/HCl used in CVG [1, 2]. The electrochemical generation is the other method in which the electric current is used for reduction of the analyte to the volatile species in presence of mineral acid medium [3, 4]. At last, the UV-photochemical vapour generation (UV-PVG) has been used [5, 6]. It is an alternative to the two previous methods. Volatile compounds are formed under the UV irradiation in presence of low molecular weight organic acid (formic,

Published online: 26 July 2016

acetic, and propionic acid) [7–9] or other chemicals [10–12] in the UV generator. UV-photochemical generation can be combined with different detection such as AAS [13–17], AFS [10, 18–20], ICP-MS [5, 10, 18, 21, 22], ICP-OES [23, 24] or can be used as a derivatization unit for speciation analysis [20, 27–31] connected to the output of chromatographic column.

UV-photochemical generation of volatile compounds with various kinds of detection is one of the possible ways to determine arsenic [32] and also other hydride forming elements [25, 26] in the sample. This derivatization method is based on photolytic decomposition of low molecular weight organic acids (formic, acetic, propionic) to form hydrocarbons, radicals and CO_2, according to the Eq. (1) [32].

$$\mathrm{R\text{-}COOH} \xrightarrow{h\nu} \mathrm{R}^{\bullet} + {}^{\bullet}\mathrm{COOH} \rightarrow \mathrm{RH} + \mathrm{CO_2} \quad (\mathrm{R} = \mathrm{C}_n\mathrm{H}_{2n+1}, n = 0, 1, 2). \tag{1}$$

Hydrocarbon radicals are taken up by trivalent arsenic to form stable substituted compounds as shown in Eq. (2) [32].

$$3\mathrm{RCOOH} + \mathrm{H_3AsO_3} \xrightarrow{h\nu} 3\mathrm{CO_2} + \mathrm{R_3As} + 3\mathrm{H_2O} \quad (\mathrm{R} = \mathrm{C}_n\mathrm{H}_{2n+1}, n = 0, 1, 2). \tag{2}$$

For a spontaneous release of the compounds generated from a solution it is necessary that the products formed are sufficiently volatile. Such compounds containing the determined element are formed by photolysis of formic acid, acetic acid, and propionic acid. Volatile arsenic species generated by UV irradiation of aqueous solutions of arsenite in various low molecular weight carboxylic acid media are identified in article [32]. Identification of arsenic alkylation products by UV irradiation in acetic acid solution was reported in detail in paper [33]. The authors concluded that the photoalkylation of arsenic in acetic acid by UV irradiation has not only formed trimethylarsine, but also a whole range of aqueous soluble species. They also presumed similar processes for other low molecular weight carboxylic acid media.

The aim of this work was to develop a method of UV-photochemical generation of volatile compounds (UV-PVG) employable for determination of arsenic with atomic absorption detection in an externally heated quartz tube (QT-AAS) in a flow injection analysis (FIA) mode. The method is based on a reaction of formic acid with arsenic compounds by UV irradiation. We looked for ions or compounds influencing the signal measured, especially in a positive way. The suitable reaction modifier was chosen based on these results. The developed analytical method was successfully used for determination of arsenic (III) compounds in model samples as a basis for the future investigation considering of speciation analysis.

Results and discussion

It was experimentally proved that evaluation from peak heights was more precise than evaluation from peak areas in FIA mode for this study. The peaks were usually high, narrow and nearly symmetrical with very small influence of analytical zone dispersion.

Optimization of working conditions

First, it was necessary to find the optimum conditions for UV-photochemical generation of volatile arsenic compounds. Following key parameters were optimized: the volume of sampling loop, the length of irradiated reaction coil (UV-photoreactor), the flow rate of carrier liquid, the concentration of formic acid in this solution, the flow rate and input/inlet position of gases (Ar, H_2), and the temperature of the atomizer. The optimum experimental conditions were found to achieve a sufficient signals as well as the highest possible efficiency of the generation of volatile arsenic compounds. FIA instrumental set-up is introduced in Experimental part of this paper and it is shown in Fig. 6. The list of initial conditions is shown in Table 1. Each of these parameters was optimized to achieve the highest peak in FIA mode.

Influence of carrier gas flow rate connected before sampling valve

Argon was introduced as the carrier gas into the apparatus through PTFE tube and peristaltic pump. Its flow rate was controlled by the choice of suitable diameter of Tygon pumping tube. This kind of carrier gas introduction was used for segmentation of flow and prevention of spread zones of the injected sample. The tube with inner diameter of 0.51 mm and carrier liquid flow rate of 0.33 $cm^3\ min^{-1}$ were chosen as optimum values of these parameters for further measurements.

Effect of carrier gas (Ar) total flow rate

It was found experimentally that the presence of carrier gas is necessary for the efficient release of volatile compounds of arsenic from a liquid phase and for their quantitative transport into the atomizer. The effect of the carrier gas total flow rate was studied from 16 to 110 $cm^3\ min^{-1}$. It had a significant effect not only on the gas–liquid separation and on the analyte transport but the carrier gas flow rate also influenced the UV-PVG. The baseline was not stable at low values of flow rate of argon. It could have several causes. The explanation could be connected with the different composition of the gaseous phase transported from the gas–liquid separator; mixing the carrier gas with

Table 1 Working conditions for determination of arsenic by FIA-UV-PVG/QT-AAS

Parameter	Initial value	Optimized value
Total flow rate of carrier gas Ar/ cm^3 min^{-1}	50	24
Flow rate of reaction gas H_2/cm^3 min^{-1}	25	30
Flow rate of carrier liquid/cm^3 min^{-1}	2	2
Length of reaction coil/cm	250	250
Volume of injected sample/mm^3	600	600
Concentration of HCOOH/mol dm^{-3}	1.5	0.75
Temperature of atomizer/°C	950	950

reaction gas and with the oxygen diffused from atmosphere surrounding the atomizer (insufficiently shielded by Ar). The effect of argon flow rate on peak width (approximately 30 s) was not significant, whereas peak height was influenced strongly. The absorbance increased rapidly with decreasing argon flow rate. Figure 1 shows the effect of carrier gas flow rate on the signal of arsenic. The total flow rate of 24 cm^3 min^{-1} Ar was chosen for all the following experiments as the optimum.

Effect of reaction gas (H_2) flow rate

The presence of hydrogen radicals is necessary for UV-photochemical generation of volatile compounds of arsenic as well as for their atomization in the quartz tube atomizer. Therefore, it was investigated if added hydrogen into the UV-photoreactor can increase the signals (probably as well as the reaction rate) in FIA arrangement. Attained dependence is shown in Fig. 2. The absorbance first increased with the ascending hydrogen flow rate starting at 10 cm^3 min^{-1}, reached the maximum at 30 cm^3 min^{-1}, and then slowly decreased for higher flow rates. Reaction of the excess of hydrogen in the atomizer with atmospheric oxygen provided radicals as well as water and changed the atomization conditions. These changes resulted in a decrease of measured peak heights while the width was approximately constant. The introduction of the inert carrier gas instead of the reaction gas at the same flow rate by this channel did not lead to any increase of peaks.

Dependence of the absorbance (peak height) on concentration of formic acid

Aqueous formic acid solution served as carrier liquid in this analytical method. Therefore, concentration of formic acid was the next optimized parameter. It was a key parameter for UV-photochemical generation because it is a source of radicals. The appropriate concentration of formic acid is needed for generation of volatile compounds of arsenic. The samples of arsenite were prepared in the solutions containing the same concentration of formic acid, as was the concentration in carrier liquid. The best signal absorbance was attained for 0.75 mol dm^{-3}. Therefore, this concentration of formic acid was applied as an optimized condition for following experiments (Fig. 3). The optimum working conditions for the determination of arsenic by UV-photochemical generation with AAS detection are listed in Table 1.

Effect of selected compounds

A hollow cathode lamp was replaced by a Superlamp at the beginning of this part of the study with the aim to improve the signal/noise ratio.

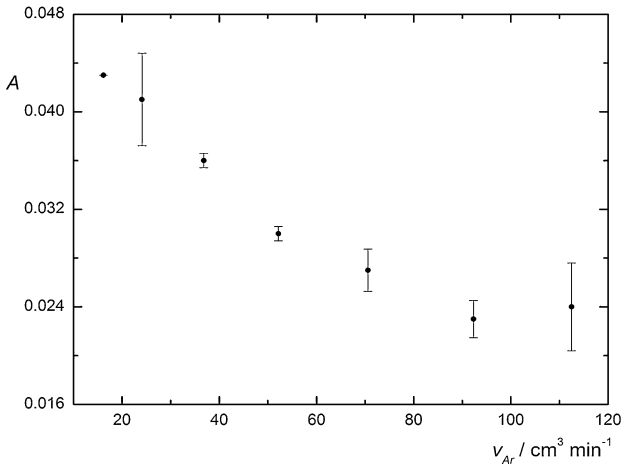

Fig. 1 Effect of argon total flow rate on the absorbance signal. Concentration of arsenic: 0.4 mg dm^{-3}. Experimental conditions are given in Table 1

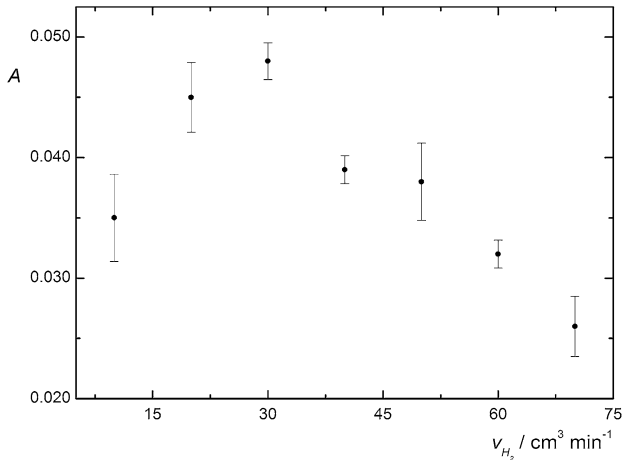

Fig. 2 Effect of hydrogen flow rate on absorbance. Concentration of arsenic: 0.4 mg dm^{-3}. Other experimental conditions are given in Table 1

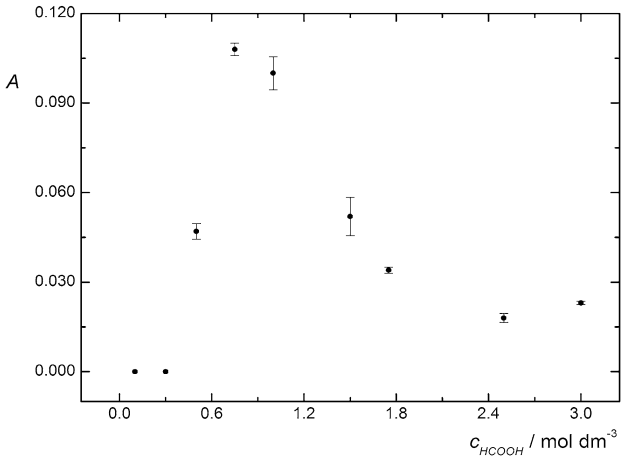

Fig. 3 Effect of concentration of formic acid (in carrier liquid). Concentration of arsenic: 1 mg dm^{-3}. Other experimental conditions are given in Table 1

It is well known that some compounds can influence the UV-photochemical generation used for determination of arsenic. The effect of fifteen various compounds or ions on the arsenic determination by UV-PVG-AAS was investigated with the intended purpose to find a suitable reaction modifier which could make UV-PVG analytically usable. It was not the aim to do a detailed overview of interferences but just to find such substances and to compare their positive effect and experimental conditions at which they would increase the arsenic absorbance. The concentration of arsenic of 1 mg dm^{-3} was used for this study in model samples as well as the appropriate concentration of the compounds or ions tested in the range from 10^{-3} to 10^{2} - mg dm^{-3}. Consequently, the signals of model samples enriched by various concentrations of selected compounds were measured.

Following substances were tested: transitions metals (Fe, Ni, Co, and Cu as common interferents for hydride generation), organic compounds (ethanol, 2-mercaptoethanol, triethanolamin, and acetonitrile as possible solvents or additives for HPLC with the intended use in speciation analysis), and other compounds [nitric acid, hydrochloric acid, sulfuric acid, titanium dioxide, L-cysteine, Se(IV), and Bi(III)] selected on the base of facts presented in published articles related to UV-PVG or to hydride generation. For example, 2-mercaptoethanol is used for UV-photochemical generation of mercury cold vapour because it increases the signal measured significantly [27, 34].

The tested compounds can be divided into three groups according to the results attained: compounds with a negative effect (in following text negative interferents), minimum interfering species and compounds with a positive effect on arsenic signal (positive interferents or potential reaction modifiers).

The higher was the concentration of each negative interferent the more intensive was the depression of arsenic signal. Negative interferents group includes: Ni(II) reducing the absorbance of arsenic more than three times from 0.01 mg dm^{-3}, Cu(II) ions which significantly reduced the signal from 0.1 mg dm^{-3}, chloride ions reducing absorbance more than a half from 0.01 mg dm^{-3}, and 2-mercaptoethanol which was the most significant negative interferent and its concentration higher than 0.005 mg dm^{-3} caused a decrease of absorbance to zero.

The minimum interfering species like nitric acid, Fe(III), ethanol, sulfate ions, titanium dioxide, and L-cysteine had just an insignificant effect on the signal of As(III) in range of 0.01–1 mg dm^{-3}. About one (HNO_3, Fe(III), ethanol, L-cysteine) or two (sulfate ions, TiO_2) order higher concentration of these substances (compared to the As(III) concentration) in model sample solutions had negative impact on arsenic absorbance which was proportional to its concentration too.

The positive interferents group includes: Co(II) increasing absorbance about 65 % in the concentration range from 0.01 to 0.1 mg dm^{-3}, acetonitrile with a positive effect (about 50 %) in the entire concentration range (from 0.005 to 100 mg dm^{-3}), triethanolamine which had a significant positive influence (about 20 %) also from 0.01 to 0.1 mg dm^{-3}, Se(IV) which interfered positively (about 35 %) in the range from 0.005 to 0.1 mg dm^{-3}, and bismuth ions which increased the absorbance most significantly at 10 mg dm^{-3}. A very strong (up to 100 %) negative influence on arsenic absorbance was observed at concentrations of these substances higher than for above listed concentration ranges with positive effect.

The most interesting results were obtained with Bi(III). The enhancement of arsenic absorbance was about 86 % in the presence of 10 mg dm^{-3} of Bi(III). This was the best result achieved. For this reason, Bi(III) was chosen as the most suitable reaction modifier for the determination of arsenic using UV-photochemical generation of volatile compounds and AAS. The influence of Bi(III) on arsenic absorbance measured is displayed in Fig. 4 as a very important example of attained dependences. The concentration of Bi(III) is plotted in a logarithmic scale on horizontal axis and the normalized absorbance (with the reference value measured previously for 1 mg dm^{-3} As(III) without the presence of any studied compound indicated by a horizontal line) on vertical axis in Fig. 4. Similarly as chloride ions or Ni(II), Bi(III) caused peak height decrease more than a half since a concentration of 5–10 μg dm^{-3}. Attained peaks became the same height as without the presence of Bi(III) when increasing its concentration to 1 mg dm^{-3}. The addition of Bi(III) above this concentration lead to increase of arsenic signal. The

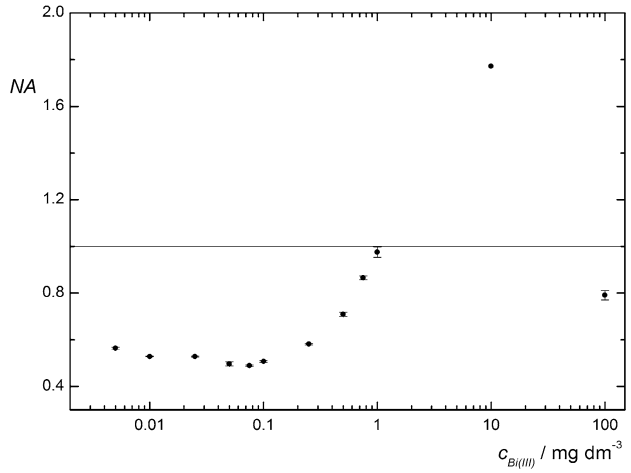

Fig. 4 Effect of Bi(III) concentration on the normalized absorbance (NA) of As. Concentration of arsenic: 1 mg dm^{-3}. Used optimum experimental conditions are listed in Table 1

presence of 100 mg dm^{-3} of Bi(III) lead to decrease of arsenic signal again.

The following experiments have shown that it is not necessary to add Bi(III) into each sample solution but it is simply enough to flush the apparatus with a solution of 10 mg dm^{-3} of Bi(III) for a few minutes before the start of the measurements. This modified apparatus was consequently stable throughout the whole day of measurements. The localization and mechanism of acting would be a subject of a future investigation.

Figures of merit

The characterisation of analytical method for As(III) determination by UV-PVG/QT-AAS was performed after all the optimization experiments. First, the calibration in the concentration range from 0 to 1.6 mg dm^{-3} of As(III) was measured without previous activation by Bi(III) under the optimum working conditions. The established values of following parameters are summarized in Table 2. Limit of detection (LOD) and limit of quantification (LOQ) were calculated as the concentration causing a signal equal to three times (or ten times, respectively) the standard deviation of ten repeated measurements of the As(III) model solution with a concentration of 200 μg dm^{-3}. The repeatability was expressed as the relative standard deviation (% RSD, $n = 10$) of results for 1.5 mg dm^{-3} of As(III). The calibration dependence is depicted in Fig. 5. The linear dynamic range (LDR) was relatively wide thanks to the low sensitivity.

Second, the calibration with long term modification (after the activation of the apparatus by Bi(III) but without addition of Bi(III) into the sample solution or carrier liquid) of the apparatus was measured again in concentration interval from 0 to 1 mg dm^{-3} of As(III). For comparison of both calibration dependences please see Fig. 5. The parameters characterizing this method were determined by the same procedure as the previous. An overview of their values is given in Table 2 for easy comparison between the approach without and after the activation. The LOD and LOQ [attained for concentration of 20 μg dm^{-3} of As(III)] moved to the lower concentration level as well as LDR after the activation. On the other hand, LDR became shorter in this case. From equations of the calibration lines, the signal enhancement factor (calculated as a ratio of both sensitivities) was calculated. Its value is 10.8.

Conclusions

A simple apparatus was constructed for determination of arsenite in model aqueous solutions by flow injection analysis. UV-photochemical vapour generation connected on-line with AAS detection in externally heated quartz tube atomizer was employed in this work. However, a very poor absorbance was attained after the optimization of the experimental conditions, which are usual for UV-PVG of other elements. Therefore, fifteen selected compounds were tested with the expectation to find a suitable reaction modifier with a positive effect for UV-photochemical generation of volatile arsenic compounds.

The most positive influence on arsenic absorbance (increase of 86 %) was observed in presence of 10 mg dm^{-3} of Bi(III) in a sample. Even more interesting is that Bi(III) became evident a long term modifier of internal surface of the apparatus. The localization and mechanism of this activity would be a subject of future investigation but it is a fact that this effect persisted for all the following measurements of the day after flushing the apparatus by the Bi(III) solution. Thus it is not needed to add Bi(III) into the routine or calibration samples.

The proposed method is distinguished by a detection limit of 18 μg dm^{-3} of arsenic, by a sensitivity of 1.1×10^{-3} dm^3 μg^{-1} (nearly 11 times higher than without activation), by a repeatability of 4.5 % and by a linear dynamic range of 60–500 μg dm^{-3} under the optimum conditions and after the activation by bismuth(III).

Relevant data for comparison of method characteristic (combination of UV-PVG with QT-AAS) were not found in available published articles. For partly comparison, limit of detection of 0.09 μg dm^{-3} (peak height) was reported for determination of arsenic by high-pressure liquid flow injection to high-resolution continuum source hydride generation atomic absorption spectrometry [35]. Just about one order lower LOD was found for arsenical speciation analysis by HPLC-(UV)-HG-AFS [29]. About one and half order lower LOD reached by the same volatile compounds

Table 2 Figures of merit for determination of As(III) using UV-PVG/QT-AAS without and after activation of the apparatus by Bi(III)

	Without activation	After activation
LOD/μg dm^{-3}	89	18
LOQ/μg dm^{-3}	300	60
Sensitivity/dm^3 μg^{-1}	1.1×10^{-4}	1.1×10^{-3}
Repeatability (RSD)/%	1.9	4.5
LDR/μg dm^{-3}	300–1500	60–500

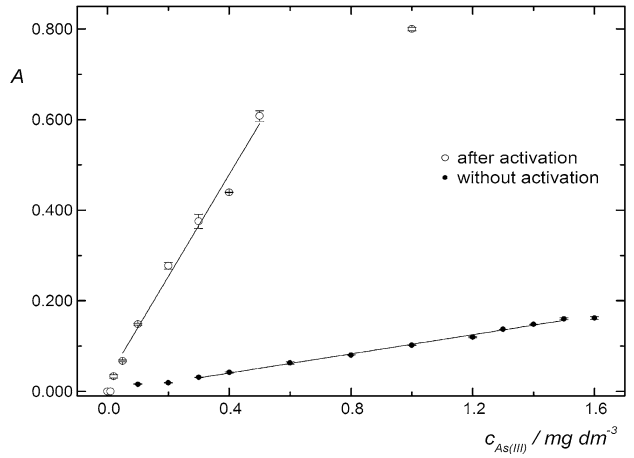

Fig. 5 Calibration dependences of As(III) without and after activation of the apparatus by Bi(III). Used optimum experimental conditions are listed in Table 1

generation technique (UV-PVG) and atomic fluorescence detection [19]. About two orders lower detection limit was achieved for HG-AAS with preconcentration in a cryotrap [17]. It is necessary to mention that AFS is much more sensitive than AAS and cryotrapping can also improve LOD significantly.

On the other hand, no signal was observed for concentration higher than 5 μg dm^{-3} of 2-mercaptoethanol, an organic additive with the highest negative effect of all the studied compounds.

This work shows that UV-photochemical generation of arsenic volatile species is applicable as well as the other techniques of volatile compounds generation. A comparable sensitivity with the other vapour generation techniques, simplicity of the apparatus and an effortless measurement procedure are the advantages of this approach, which is also environmentally friendly.

Moreover, an applicability of this approach for arsenic speciation seems to be possible in future. It was confirmed experimentally that L-cysteine which is often used for sample preparation does not interfere and that acetonitrile (potential mobile phase component) even increase the signal of arsenic in studied concentration range.

Experimental

An analytical method for determination of arsenic using its UV-photochemical volatile compound generation was developed in this work. The arsenic volatile compounds were detected by atomic absorption spectrometer Varian SpectraAA-300A (Varian, Australia) after the atomization in a conventional T-shaped quartz tube (QT-AAS) which was externally heated to 950 °C (RMI, CZ). An arsenic hollow cathode lamp (Heraeus, Germany, current of 10 mA, $\lambda = 193.7$ nm) and a Superlamp (Photron, current of 18 mA, boosted by 20 mA, $\lambda = 193.7$ nm) served as sources of radiation. The used quartz tube atomizer (atomization tube had conventional dimensions) was unique because it had an integrated gas–liquid separator (GLS) with forced outlet at the ending of the inlet arm. The GLS inner volume was approximately 7 cm^3. Both these parts were laboratory-made as one piece of quartz. A scheme of the instrumental set-up for UV-PVG/QT-AAS employed in flow injection mode is depicted in Fig. 6.

Arsenic volatile compounds were generated in a flow-through UV-photoreactor consisting of a 2.5 m-long Teflon (PTFE) tube (1.0 mm ID, 1.4 mm OD) wrapped around a source of UV-radiation. A low-pressure mercury UV bench lamp (254 nm, 20 W, dimensions 610 × 152 × 108 mm) (purchased from Ushio, Japan) was used as the source of UV-radiation.

Formic acid was pumped to the UV-photochemical reactor using a MasterFlex programmable peristaltic pump with an eight-channel Ismatec head (Cole-Parmer, USA). The sample was injected into the flow of carrier liquid by a six-way injection valve via a 600 mm^3 injection loop. Hydrogen was introduced to the apparatus before the UV-photochemical reactor and its flow rate was controlled by a flowmeter (Cole-Parmer, USA, model 32907-67, range 0–1000 cm^3 min^{-1}). A stream of argon was introduced to the apparatus into two different places (before the six-way injection valve and into the gas–liquid separator). A flowmeter (Cole-Parmer, USA, model N112-02) was used for regulation of total argon flow rate. Tygon and Teflon tubes of various inner diameters and lengths were used as a connection material in the apparatus.

Reagents and samples

Deionized water prepared in a $MilliQ_{plus}$ system (18.2 MΩ cm; Millipore, USA) was used for dilution of all the solutions. The stock solution of As(III) was prepared by dissolving the appropriate amount of arsenic trioxide (>99.5 %, Sigma–Aldrich, USA) in slightly alkaline (solid KOH—89.0 %, Lach-Ner, CZ) solution. Formic acid (HCOOH, ≥98 %, Sigma–Aldrich, USA) was used as UV-

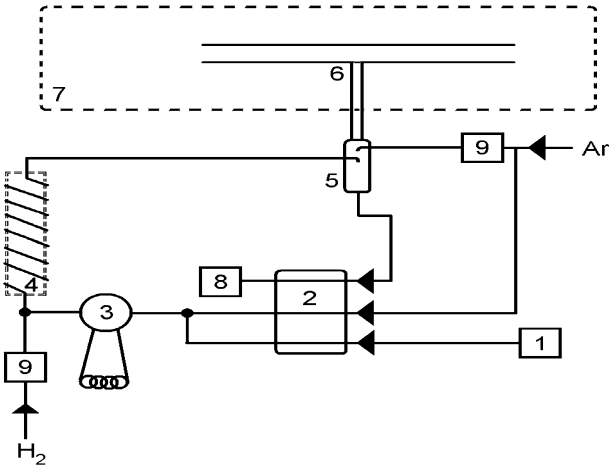

Fig. 6 A scheme of the instrumental set-up for UV-PVG/QT-AAS (FIA). *1* reservoir bottle with solution of HCOOH, *2* peristaltic pump, *3* six-way injection valve, *4* UV-lamp with reaction coil, *5* gas–liquid separator with forced outlet integrated to, *6* externally heated quartz tube atomizer, *7* AAS, *8* waste bottle, *9* gas flow controller

photochemical reaction agent and its solutions were prepared fresh daily. Argon (99.998 %; Linde Gas, CZ) was used as the inert carrier gas during all the experiments. Hydrogen (99.998 %; Linde Gas, CZ) was used as the reaction gas during all the experiments.

The solutions of the studied compounds or ions were prepared from standard solution of Fe(III) (1002 ± 2 mg dm^{-3}, Merck, Germany), Co(II) (1002 ± 2 mg dm^{-3}, Merck, Germany), Ni(II) (1000 ± 5 mg dm^{-3}, Analytika, CZ), Cu(II) (1000 ± 5 mg dm^{-3}, Analytika, CZ), Se(IV) (1000 ± 2 mg dm^{-3}, Analytika, CZ), Bi(III) (1001 ± 5 mg dm^{-3}, Merck, Germany), SO_4^{2-} (1000 ± 2 mg dm^{-3}, Merck, Germany) and Cl^- (1000 ± 2 mg dm^{-3}, Merck, Germany), or diluted from stock solutions of HNO_3 (≥65 %, Merck, Germany), ethanol (≥99.5 %, Merck, Germany), 2-mercaptoethanol (≥99.0 %, Sigma-Aldrich, USA), triethanolamine (≥98 %, Sigma-Aldrich, USA), acetonitrile (≥99.8 %, Sigma-Aldrich, USA) or by dissolving of solid L-cysteine hydrochloride monohydrate (≥98 %, Sigma-Aldrich, USA), TiO_2 (≥99.5 %, size of nanoparticles ~21 nm, Aldrich, USA).

Determination of As(III) by UV-PVG/QT-AAS

Samples prepared in formic acid medium were injected by an injection valve via a 600 mm^3 injection loop into the flow of carrier liquid (a solution of formic acid). Sample zone together with carrier liquid was pumped into the UV-photoreactor where arsenic volatile compounds had been formed under the UV irradiation. The reaction mixture with generated volatile products was transported into a gas–liquid separator. The liquid phase was pumped into the waste while the gaseous phase, which was flushed out by a stream of argon, entered the atomizer.

Acknowledgments The authors acknowledge for financial support from the Charles University in Prague: GAUK152214, Project SVV260317 and Project UNCE204025/2012.

References

1. Marschner K, Musil S, Dědina J (2015) Spectrochim Acta 109:16
2. Rybínová M, Červený V, Hraníček J, Rychlovský P (2015) Microchem J 124:584
3. Sturgeon RE, Mester Z (2002) Appl Spectrosc 56:202
4. Červený V, Rychlovský P, Hraníček J, Šíma J (2009) Chem List 103:652
5. Quadros DPC, Borges DLG (2014) Microchem J 116:244
6. Silva CS, Oreste EQ, Nunes AM, Vieira MA, Ribeiro AS (2012) J Anal At Spectrom 27:689
7. Guo X, Sturgeon RE, Mester Z, Gardner GJ (2003) Anal Chem 75:2092
8. Guo X, Sturgeon RE, Mester Z, Gardner GJ (2003) Appl Organomet Chem 17:575
9. Guo X, Sturgeon RE, Mester Z, Gardner GJ (2003) Environ Sci Technol 37:5645
10. Zheng C, Wu L, Ma Q, Lv Y, Hou X (2008) J Anal At Spectrom 23:514
11. Hou X, Ai X, Jiang X, Deng P, Zheng C, Lv Y (2012) Analyst 137:686
12. Han C, Zheng C, Wang J, Cheng G, Lv Y, Hou X (2007) Anal Bioanal Chem 388:825
13. Zheng C, Sturgeon RE, Hou X (2009) J Anal At Spectrom 24:1452
14. Figueroa R, García M, Lavilla I, Bendicho C (2005) J Spectrochim Acta 60:1556
15. Nóbrega JA, Sturgeon RE, Grinberg P, Gardner GJ, Brophy CS, Garcia EE (2011) J Anal At Spectrom 26:2519
16. Matoušek T, Hernández-Zavala A, Svoboda M, Langrová L, Adair BM, Drobná Z, Thomas DJ, Stýblo M, Dědina J (2008) Spectrochim Acta 63:396
17. Musil S, Matoušek T (2008) Spectrochim Acta 63:685
18. Li H, Luo Y, Li Z, Yang L, Wang Q (2012) Anal Chem 84:2974
19. Zheng C, Ma Q, Wu L, Hou X, Sturgeon RE (2010) Microchem J 95:32
20. Cai Y (2000) Trend Anal Chem 19:62
21. Sun YC, Chang YC, Su CK (2006) Anal Chem 78:2640
22. Shih TT, Hsu IH, Wu JF, Lin CH, Sun YC (2013) J Chromatogr A 1304:101
23. Zheng C, Sturgeon RE, Brophy CS, He S, Hou X (2010) Anal Chem 82:2996
24. Santos EJ, Herrmann AB, Santos AB, Baika LM, Sato CS, Tormen L, Sturgeon RE, Curtius AJ (2010) J Anal At Spectrom 25:1627
25. Guo X, Sturgeon RE, Mester Z, Gardner GJ (2004) Anal Chem 76:2401
26. Sturgeon RE, Willie SN, Mester Z (2006) J Anal At Spectrom 21:263
27. Yin Y, Qiu J, Yang L, Wang Q (2007) Anal Bioanal Chem 388:831
28. Quadros DPC, Campanella B, Onor M, Bramati E, Borges DLG, DÚlivo A (2014) Spectrochim Acta Part B 101:312
29. Šlejkovec Z, Kápolna E, Ipolyi I, Elteren JT (2006) Chemosphere 63:1098

30. Francesconi KA, Kuehnelt D (2004) Analyst 129:373
31. Schaeffer R, Francesconi KA, Kienzl N, Soeroes C, Fodor P, Váradi L, Raml R, Goessler W, Kuehnelt D (2006) Talanta 69:856
32. Guo X, Sturgeon RE, Mester Z, Gardner GJ (2005) J Anal At Spectrom 20:702
33. McSheehy S, Guo X, Sturgeon RE, Mester Z (2005) J Anal At Spectrom 20:709
34. Yin Y, Liu J, He B, Shi J, Jiang G (2009) Microchim Acta 167:289
35. Hesse S, Ristau T, Einax JW (2015) Microchem J 123:42

Spectrochimica Acta Part B 134 (2017) 98–104

Contents lists available at ScienceDirect

Spectrochimica Acta Part B

journal homepage: www.elsevier.com/locate/sab

Analytical note

Flow injection determination of Se in dietary supplements using TiO_2 mediated ultraviolet-photochemical volatile species generation

E. Nováková *, O. Linhart, V. Červený, P. Rychlovský, J. Hraníček

Charles University, Faculty of Science, Department of Analytical Chemistry, Albertov 6, Prague 2 CZ 128 43, Czech Republic

ARTICLE INFO

Article history:
Received 21 February 2017
6 June 2017
Accepted 6 June 2017
Available online 15 June 2017

Keywords:
Dietary supplements
Selenite
Selenate
UV-photochemical volatile species generation

ABSTRACT

This paper proposes a method for determination of selenium content in samples of dietary supplements using TiO_2 mediated UV-photochemical vapor generation with quartz furnace atomic spectrometric detection. The flow-injection method was optimized for determination of selenium in the form of selenite or selenate ions. The limits of detection of the proposed method are 0.89 ng mL^{-1} and 0.68 ng mL^{-1} for selenite and selenate, respectively. Extraction in neutral medium was used for the leaching of selenate and NaOH solution was used for the leaching of selenite. The methods accuracy was verified against the declared amounts of Se in five different samples of over-the-counter dietary supplements and on NIST SRM 3280. The method was also compared to results achieved with determination by electrothermal atomization atomic absorption spectrometry following microwave decomposition. The recovery of selenium during sample preparation was tested by spiking the tablets prior to extraction and estimated to be approximately 100%. An interference study has been carried out to estimate the effect of concomitant elements on the methods accuracy.

1. Introduction

Selenium is an important element with effects on human health. Currently, it is considered an essential trace element but with a very narrow therapeutic range. Se effects on mammals have been re-evaluated several times in the past; it had been considered toxic and carcinogenic until the discovery of selenoamino acids in 1966 [1]. Se is included in human body in proteins with a wide variety of biochemical effects but the cancer protective function is supposed to be caused by Se-containing glutathione peroxidase enzyme decreasing oxidative stress [2]. On the other hand, high doses of Se can cause acute toxic effects and cell apoptosis through the production of reactive oxygen species i.e. through an inverse effect [3]. In addition, Se plays an active role in testosterone synthesis, production of thyroid hormones through iodothyronine deionidase enzyme and is also associated with normal functioning of immune system [4,5]. Chronic Se toxicity in humans results in selenosis, which is characterized by hair loss, nail brittleness, garlic breath, gastrointestinal disturbances, and abnormal functioning of the nervous system [6]. Recent publications also mention an increased risk of type II diabetes associated with increased Se consumption through disruption of insulin signaling cascade [7].

Particularly the possibility that selenium may act as cancer protective agent has led to a widespread marketing of Se containing dietary supplements [8]. However, its complicated behavior in the living organism requires strict control of its consumption. Several studies have tried to determine whether the manufacturer-declared Se contents in dietary supplements can be believed. Some authors lean towards confirming the declared values sometimes with reservations towards the identity of the organic species [8–11]. Other authors raise a warning finger that the real contents may in some cases be different from the manufacturer-declared values [12,13].

Determination of selenium in dietary supplements containing selenized yeast usually requires speciation analysis and is carried out using HPLC separation with atomic fluorescence spectrometric detection (AFS) [14,15] or mass spectrometric detection (MS) [8,16–19]. The determination of total Se content in dietary supplements has so far been determined by electrothermal atomic absorption spectrometry (ETAAS) [9,20], inductively coupled plasma optical emission spectrometry [11] and inductively coupled plasma mass spectrometry [8]. Several works also proposed using chemical hydride generation methods to remove spectral interference from the complicated dietary supplement matrices [10,12,20,21].

Ultraviolet photochemical generation (UV-PVG) is a volatile species generation method based on the use of UV radiation and its application for the determination of Se was pioneered by Guo et al. in 2003 [22–24]. Samples are irradiated dissolved in a low molecular weight organic acid with or without the use of photocatalyst [25,26]. It is known that TiO_2 can catalyze the reduction of selenate to a volatile compound in the presence of formic acid and UV radiation [27–31]. Until now UV-PVG

* Corresponding author.
E-mail address: eliska.novakova@natur.cuni.cz (E. Nováková).

http://dx.doi.org/10.1016/j.sab.2017.06.007
0584-8547/

has been used for the determination of Se in the following samples: seawater [32] and modified seawater samples [33], biological samples [34] and once for the determination of Se(IV) in dietary supplements [35].

Nevertheless, the method published by Rybínová et al. had several drawbacks like being time consuming and requiring complicated sample preparation due to an off-line prereduction of the selenate ion in 6.0 M HCl [35]. This paper presents an improved UV-PVG method utilizing TiO_2 photochemical catalyst and flow injection set up for the determination of Se in samples of dietary supplements. This is the first time that dietary supplements have been analyzed using TiO_2 mediated UV-photochemical generation of volatile Se species. No prereduction of Se(VI) during the sample preparation was necessary. The photochemical catalyst permitted an on-line reduction of Se(VI) during the generation of volatile compounds. The determination has been carried out in flow injection set-up, which reduced the sample consumption and increased the sample throughput.

2. Experimental

2.1. Instrumentation

A schematic diagram of the instrumental set-up is shown in Fig. 1. The flow system consisted of a MasterFlex peristaltic pump (Cole-Parmer, USA) driving the solutions, a low pressure six port injection valve (IDEX, USA) with 200 μL PTFE injection loop, a flow-through UV photoreactor and glass gas-liquid separator (volume 6.2 mL) with forced outlet. A second peristaltic pump (VD ČSAV, Czech Republic) was used to remove the waste solution. The photoreactor consisted of 3.4 m long PTFE tube (i.d. 0.8 mm/o.d. 1.58 mm, Sigma-Aldrich, USA) wrapped around a low pressure mercury UV lamp (253.7 nm, 20 W, dimensions 610 × 152 × 108 mm, USHIO, Japan). The lamp and its reflective housing (Upland, USA) were covered by a lid made from hard cardboard and aluminum foil to protect the analyst from exposure to UV rays. Argon (99.998% purity, Linde, Czech Republic) was introduced into the apparatus prior to the reactor as a carrier gas. Hydrogen (99.90% purity, Linde, Czech Republic) was introduced between the gas-liquid separator and quartz furnace atomizer to facilitate atomization. Digital mass flow controllers for flow rates 1.00–100 mL min^{-1} and 0.50–50 mL min^{-1} (Cole-Parmer, USA) were used to control the flow rates of Ar and H_2 respectively. Tygon tubes of various diameters were used for pumping of solutions, PTFE tubing and PP connecting pieces were used in fluid pathways.

A Solaar 939 AA spectrometer equipped with Se hollow cathode lamp (Heraeus, run at 12 mA) has been used for measurement of atomic absorption. The measurements were carried out at the 196.0 nm line (bandwidth 0.5 nm). Atomization of the evolved volatile products was carried out in an externally heated quartz furnace atomizer (T-shaped, inlet arm length 700 mm, optical arm length 119 mm, internal diameter of the atomizer tube at the position of radical cloud 7.5 mm, RMI, Czech Republic). The atomizer was heated to 950 °C. A combined ultrasonic bath and heater (Elmasonic S, purchased from P-lab, Czech Republic) has been used for the extraction of Se from samples.

Microwave digestion system CEM MDS 2000 (CEM, USA) with pressure sensor was used for total digestion of samples for determination by ETAAS. A HR-CS-AAS ContrAA 700 (Analytik Jena, Germany) equipped with a transversally heated graphite furnace atomizer with integrated platform was used for the determination of Se in samples following total digestion of the samples. The results were used as reference for validation of the proposed method.

2.2. Reagents

Deionized water prepared by the $MilliQ_{Plus}$ system (Millipore, USA) was used throughout the measurements. Formic, acetic and propionic acids (all from Sigma-Aldrich, USA) were tested for the preparation of photochemical reagents; acetic acid (>99.8) diluted to 0.5 mol L^{-1} solution was used in Se determination. TiO_2 suspension (>99.5% purity, nanocrystalline, Sigma-Aldrich, USA) prepared in 0.5 mol L^{-1} acetic acid served as photocatalyst. Selenite and selenate standards with concentration of Se 100 mg L^{-1} were prepared from sodium selenite pentahydrate and sodium selenate decahydrate, respectively (both from Sigma-Aldrich, USA). Sodium hydroxide solution used in extraction was prepared from sodium hydroxide micro pearls (p.a., Lachner, Czech Republic). Standard solutions of Zn(II), Fe(III), Cu(II), Cr(III), Mn(II), Mo(VI), As(III), Sb(III), Ni(II) and Te(IV) prepared in nitric acid (1000 mg L^{-1}, all from Analytika, Czech Republic) were used as stock solutions for interference study. Stock solutions of Ca(II) and Mg(II), were prepared from their nitrate salts and solution of iodide from KI (all from Lachner, Czech Republic). Nitric acid (Merck, Germany) was used for wet digestion of samples. Se stock solution in 2.0% HNO_3 (Analytika, Czech Republic) was used for preparation of calibration standards in ETAAS measurements. All reagents were of analytical or higher purity.

2.3. Composition of samples

Samples were in the form of tablets or capsules. They were denoted A-E, where samples A and D contained Se in the form of sodium selenite and samples B, C and E sodium selenate. The declared Se contents in the analyzed samples ranged from 25 to 55 μg per tablet. We used the

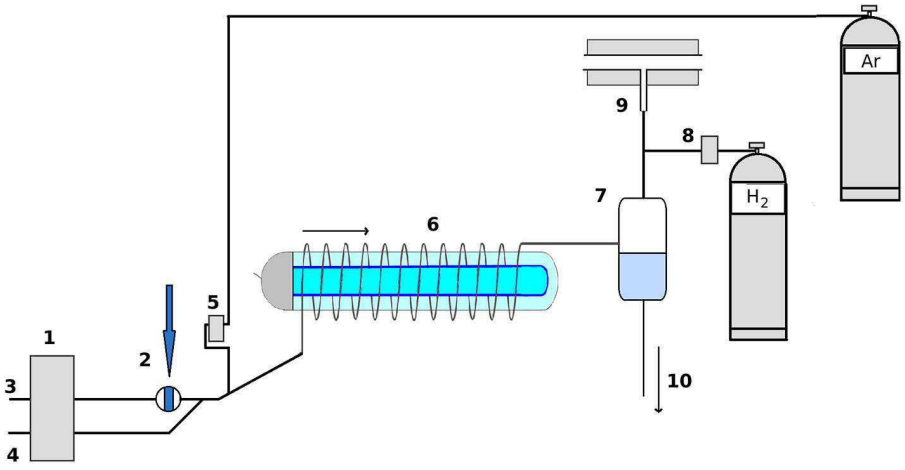

Fig. 1. Experimental set-up for UV-PVG of Se volatile species. 1 – peristaltic pump, 2 – low pressure six-port injection valve, 3 – acetic acid, 4 – photocatalyst suspension, 5 – argon flow rate regulation, 6 – UV-photochemical reactor, 7 – gas liquid separator with forced outlet, 8 – hydrogen flow rate regulation, 9 – externally heated quartz furnace atomizer, 10 – removal of waste solution.

values declared by manufacturers and the contents determined by ETAAS as reference.

NIST SRM 1640a was used for the verification of the accuracy of the UV-photochemical vapor generation. This certified reference material is a semi-synthetic acidified water sample with mass fractions and mass concentrations assigned for 29 elements, 22 of which were gravimetrically added. The solution contains nitric acid at a volume fraction of approximately 2%.

2.4. Preparation of samples of dietary supplements

A suitable extraction method compatible with UV-PVG was necessary to apply the proposed UV-PVG method for the determination of Se in dietary supplements. Use of enzymatic digestion of samples was avoided in order to simplify the extraction procedure. All tablets were weighed and ground to fine powder prior to extraction. The extraction of Se using acetic acid or NaOH was carried out by adding 15 mL of 1.0 mol L^{-1} solution of the selected agent to the weighed aliquots. The sample volume was made up to 50 mL with deionized water. When using extraction at neutral pH the sample was only dispersed in deionized water. The extraction process took 30 min at 35 °C with the help of ultrasound sonication. Subsequently, the samples were filtered through syringe filter with 0.45 μm pore size and polyamide membrane (ProFill PLUS, Fisher Scientific, USA). Filtered samples were diluted 5 or 10 times (sample C during optimization of extraction medium, sample D always) with deionized water.

2.5. CRM samples preparation

The certified reference material SRM 1640a contained nitric acid in concentration sufficient to interfere during UV-PVG [23]; see Section 2.3. Therefore, it was evaporated to near dryness to reduce the nitric acid content. Exactly 40.0 mL of CRM was evaporated and the residue was diluted to 25.0 mL with deionized water. The resulting solution had pH = 2.6.

Due to concerns regarding the complicated sample matrix Se was also determined in NIST SRM 3280 - Multivitamin/Multielement Tablets. To overcome variability between tablets 15 tablets were ground and aliquots were taken to be determined as Se(IV) and Se(VI). Both extraction procedures were used because there was no indication of Se species in the reference material certificate.

2.6. Measurement procedure and evaluation of results

The acid was continuously irradiated by the UV source. Samples were injected into the acid solution and merged with TiO_2 suspension prior to passing through the UV reactor. The signal was recorded for 80 s after sample injection. Peak area was used for quantification in all measurements except for the optimization experiments, where peak height was used instead. The standard deviations in the optimization dependences are based on three successive measurements.

Dietary supplement extracts were determined using both standard addition method and comparison of sample with external calibration. External calibration curves were measured with selenate in deionized water and selenite in the solution of 0.06 mol L^{-1} NaOH to compensate for the effect of NaOH in the sample extracts (corresponds to five times diluted sample). If not stated otherwise, two tablets were analyzed in triplicate and the mean value and SD were calculated from the total of six measurements.

The CRMs and samples used in extraction study were analyzed only by standard addition method. The calibration curve for standard addition was constructed from five points, namely diluted sample and four standard additions. Each point was mean of three replicate measurements; however the mean value and SD of the result (see Table 2 and Section 3.6) correspond to two analyzed tablets.

Interference study was carried out comparing the absorbance of model samples containing 150 ng mL^{-1} Se and a known amount of interferent with reference sample containing only Se. Each solution in the interference study was measured in triplicate.

2.7. Analysis of samples by ETAAS as a reference method

Reference measurement of Se content in the samples was carried out using microwave digestion of samples in HNO_3 and subsequent determination using ETAAS. A tablet was weighed, ground and a sample portion of <0.4 g was transferred to a PTFE digestion vessel with 5.0 ml of concentrated nitric acid. The digestion program was following: 20 min at 40% MW power, 10 min at 80% MW power, 10 min at 100% MW power. Samples were diluted as necessary by 2.0% HNO_3. The temperature program used for the determination of Se by ETAAS was taken from the built-in cookbook of the HR-CS-AAS instrument.

2.8. Evaluation of extraction

Se recovery from the matrix was tested on two selected samples (B, D) with different species and Se content. The aim was to determine whether the sample matrix does not limit the dissolution of Se through adsorption. A tablet was weighed, ground, divided in halves and one half from each ground tablet was analyzed without spiking while the other ground tablet was spiked by standard solution prior to extraction. The additions corresponded to 33 μg of Se in the form of sodium selenate solution (sample B) or 55 μg of Se in the form of sodium selenite solution (sample D).

3. Results and discussion

3.1. Photochemical reagent and irradiation conditions

The optimization of all reaction conditions was carried out with 200 ng mL^{-1} aqueous solutions of selenite and selenate. The optimized parameters were: type and concentration of organic acid, flow rate of organic acid, concentration of TiO_2 and flow rates of Ar and H_2. The atomization temperature was set to 950 °C, which is sufficient for atomization of binary hydrides or alkylated derivatives of hydride forming elements.

Formic, acetic and propionic acids were tested as potential reagents in the concentration range 0.1–2.0 mol L^{-1} using a 3.4 m long reaction tube, total acid flow rate 3.8 mL min^{-1}, TiO_2 concentration 0.005% (m/V) and carrier gas flow rate 20.0 mL min^{-1}. Acetic acid gave higher signals than the other two acids at these conditions for the whole concentration range; the selected optimum concentration of acetic acid was 0.5 mol L^{-1} (see Fig. 2). Formic acid is generally recommended for photochemical generation of volatile selenium species in combination with TiO_2 photocatalyst [30,36–39], although acetic [31] or propionic acid can be used too [40]. To our knowledge, no studies compared the performance of TiO_2 mediated UV-PVG in formic and acetic acid yet. In non-catalyzed PVG some insight into the problem of optimum acid choice was recently published by Campanella et al. [41], who studied the effect of temperature on UV-photochemical vapor generation of volatile Se species. They found out that the use of formic acid resulted in higher sensitivity compared to acetic acid when the sample solution was preheated prior to entering the reactor while the signals achieved with acetic acid did not show temperature dependence in the range 25–50 °C.

We found during optimization of the reaction coil length that 3.4 m long reactor is sufficient corresponding to residence time of 34 s. Total acetic acid flow rate 3.0 mL min^{-1} was selected as optimum for this length of reaction coil. TiO_2 prepared in the form of suspension in the diluted organic was added downstream of the injection port; its flow rate was not optimized separately from the flow rate of acid. The ratio of TiO_2 suspension flow rate to acid flow rate was 1:3 and the flow rates given

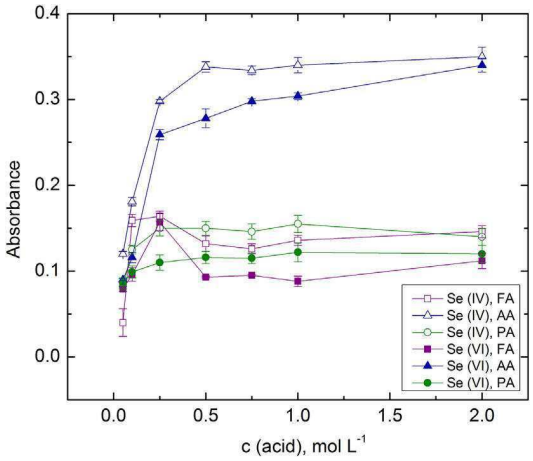

Fig. 2. Effect of type and concentration of organic acid on the sensitivity of TiO_2 mediated UV-photochemical vapor generation, 200 ng mL^{-1} Se(IV) and Se(VI), FA- formic acid, AA – acetic acid, PA – propionic acid, $n = 3$.

are total. Optimization of the TiO_2 suspension concentration over two orders of magnitude yielded highest responses of both species at the original concentration 0.005% (m/V). For the dependences of the signal on the acetic acid flow rate, the concentration of TiO_2 suspension, reaction coil length see Figs. S1–S3 (Appendix, Section S1), respectively.

3.2. Flow rates of gasses

Increasing the flow rate of Ar carrier gas led to the increase of response, however flow rates exceeding 50 mL min^{-1} led to the introduction of condensed phase from the gas liquid separator into the atomizer inlet thus increasing the standard deviation of measurements. The effect was more pronounced for Se(VI) than for Se(IV). Flow rate of 55 mL min^{-1} was selected as a compromise between the sensitivity and the repeatability of measurements. For the dependence of the signal on carrier gas flow rate see Fig. S4 (Appendix, Section S1). Flow rate of H_2 did not have pronounced effect in the region of 2.0–10.0 mL min^{-1} in concordance with the finding that it is necessary only in amount required for successful atomization of the generated volatile compound [42]. Flow rate of 4.2 mL min^{-1} was selected for further measurements.

3.3. Injected volume

The optimization of injection volume was carried out in the range of 30–500 μL. The increase of response was linear; injection volume of 200 μL was selected as it offered good sensitivity while producing symmetrical peaks suitable for integration and determination of Se from both peak height and area.

3.4. Figures of merit

Figures of merit for both Se oxidation states were determined in deionized water and selenite was also determined in 0.06 mol L^{-1} NaOH solution (see Section 2.6 for explanation). We observed that the addition of NaOH to the analyte solution did not affect the figures of merit of the method. Table 1 shows that the figures of merit for both species are comparable. The limits of detection (LOD) and quantification (LOQ) were calculated according to the IUPAC recommendations. The resulting values represent the concentration corresponding to a signal equal to three and ten times, of the standard deviation of ten repeated measurements of Se solution with a concentration below the expected LOD values; solutions containing 0.3 ng mL^{-1} of Se species were used. The LOQ defines the lower end of the linear dynamic range (LDR). The repeatability expressed as the relative standard deviation (% RSD, $n = 10$) was determined at the concentration of 125 ng mL^{-1} of the respective Se species. The sample throughput was 46 analyses per hour. The limits of detection and experimental procedures have also been compared to other published methods on the determination of Se in dietary supplements (see Table 2). The proposed method offers advantageous simplicity compared to some of the published procedures while retaining sufficiently low LOD values. These are in some cases comparable with the use of more sensitive detection techniques like AFS.

Table 1
Figures of merit of TiO_2 mediated UV-photochemical generation of Se species.

	Se(IV)[a]	Se(IV)[b]	Se(VI)[a]
LOD, ng mL^{-1}	0.79	0.89	0.68
Sensitivity, mL ng^{-1} s^{-1}	0.050	0.052	0.048
RSD, %[c]	3.1	1.5	3.3
LDR, ng mL^{-1}	3–250	3–250	2–250

[a] Determined in deionized water.
[b] Determined in 0.06 mol L^{-1} NaOH solution.
[c] Based on 10 replicate measurements of 125 ng mL^{-1} solution.

3.5. Extraction method and determined Se content

Extraction approaches using deionized water and different concentrations of acetic acid and sodium hydroxide [45] were tested and compared to find suitable pH for leaching of Se. Acidic extraction did not yield satisfactory results. Values below the declared content were found in all cases, possibly due to the amount of dissolved interfering species or low extraction efficiency. Sodium selenite could be quantitatively extracted by 0.3 mol L^{-1} NaOH and sodium selenate by water. The achieved results are shown in Table 3. The results obtained using the external calibration method and the standard addition method were compared using a paired *t*-test and no statistically significant difference was found. The results achieved using external calibration method corresponded better with the manufacturer declared values and also with the values found using MW digestion and ETAAS determination. Large standard deviations between samples were observed using both proposed UV-photochemical generation method and ETAAS (see Table 3). Notably smaller deviation was observed when analyzing the certified reference material (see Section 3.6) leading to the conclusion that this effect is associated with the matrix of the dietary supplements samples. Analysis of SRM 3280 showed that when the sample consists of a mix of more tablets the repeatability is improved. It would seem that despite the automated production process there is some variability between the tablets.

3.6. Accuracy assessment

The accuracy of the UV-photochemical vapor generation was tested by analyzing the NIST SRM 1640a certified reference material. The found value 20 ± 1 ng mL^{-1} was in good agreement with the declared value 20.13 ± 0.17 ng mL^{-1}. It is necessary to note that this approach tested only the accuracy of the vapor generation method used. The whole method was validated by determination of Se in SRM 3280. The material was processed as Se(IV) and Se(VI) as no indication regarding the nature of Se species was given. The results were 17.3 ± 0.2 μg g^{-1} (as selenite) and 17.5 ± 0.7 μg g^{-1} and therefore in good agreement with the certified value 17.42 ± 0.45 μg g^{-1}. The recovery of Se from the dietary supplement matrix was validated by carrying out experiments with spiked and non-spiked samples B and D (see Section 2.8). The recoveries counted from the difference between spiked and non-spiked samples were 107 ± 14% for sample B and 104 ± 9% for sample D. The results show that the added selenium was not adsorbed on the solid sample matrix during the sonication and filtration. The overall accuracy of the Se determination in dietary supplements was further demonstrated by the agreement of values found by the proposed and established (ETAAS) method.

Table 2
Comparison of achieved LODs and experimental procedures with other published methods dealing with the determination of Se in dietary supplements.

Method	LOD	Details	
Fl-TiO_2/UV–PVG-AAS	0.89 ng mL^{-1} for Se(IV), 0.68 ng mL^{-1} for Se(VI)	30 min extraction, sample throughput 46 runs per hour, no prereduction of Se(VI)	This work
Fl-HG-AFS	0.4 ng mL^{-1}	Microwave digestion, only Se(IV), sample throughput 50 samples/h	[21]
HPLC-MS	38–860 pg mL^{-1} for Se(IV)[a], 28–590 pg mL^{-1} for Se(VI)[a]	Reversed phase and ion-pair chromatography, Se(IV), Se(VI), Se-cystine, Se-methionine, Se-ethionine	[43]
ETAAS	0.18 μg g^{-1}	Microwave digestion of samples in HNO_3/H_2O_2, total determination of Se content	[20]
HG-AAS	0.06 μg g^{-1}	Microwave digestion of sample followed by evaporation to dryness, prereduction of Se(VI) in HCl at 95 °C, 15 min	[20]
LC-HG-UV-AFS	0.40 ng mL^{-1} for Se(IV)[b], 1.7 ng mL^{-1} for Se(VI)[b]	Se(IV), Se(VI), Se-methionine, Se-cystine, UV assisted cracking for reduction of Se(VI)	[15]
USAED-HPLC-ETAAS	437 ng g^{-1} for Se(IV), 764 ng g^{-1} for Se(VI)	Ultrasonic assisted enzymatic digestion, coupling of HPLC and ETAAS	[9]
Total reflection XRF	0.1–0.2 mg kg^{-1} of Se[c]	Solid sample analysis, total determination of Se content	[44]
HPLC-HG-AAS	10 ng mL^{-1} for both Se(IV) and Se(VI)	Separation of inorganic Se species, on-line reduction of Se(VI)	[12]
HG-HSSPME-MWP-OES	3.2 ng mL^{-1}	Alkaline dissolution using TMAH, headspace SPME for preconcentration of the generated Se hydride, only Se(IV)	[11]
RP-HPLC-ICPMS	0.06 ng mL^{-1} for Se(IV), 0.07 ng mL^{-1} for Se(VI)	Extraction using acidic mobile phase and protease XIV, Se(IV), Se(VI), Se-methionine, Se-methyl-Se-cysteine, Se-cystine	[17]
UV-PVG-AAS	0.04 ng L^{-1} for Se(IV)	Reduction of Se(VI) at 90–95 °C for 60 min, sample throughput 18 samples/h	[35]

[a] Depending on HPLC separation mode and nebuliser used.
[b] The detection limits were calculated on the basis of 3σ (σ being the residual standard deviation around the regression line) using the regression lines for the standards.
[c] LODs calculated for two different samples.

3.7. Interference study

Interference study was carried out with 50 ng mL^{-1} of Se species in the sample. The interferents were element species present in more than one of the selected dietary supplements, namely Ca(II), Mg(II), Zn(II), Fe(III), Cu(II), Cr(III), Mn(II), Mo(VI) and I(-I) in concentration ranges corresponding to the interferent-to-Se ratio content declared in the dietary supplements. Experiments were also carried out with elements, which are not approved for dietary supplements, but are likely to seriously affect UV-PVG of Se [22,39,41]: As(III), Sb(III), Ni(II), Te(IV). The recoveries are summarized in Table 4. The interference study was carried out in deionized water for Se(VI) and 0.06 mol L^{-1} NaOH for Se(IV).

The presence of interferents manifested itself by deformation of the peak signal. In general, interferences would be more pronounced when evaluating peak height than peak area. Samples without interferent were introduced randomly into the measurement sequence to determine whether the concomitants caused memory effects. No such behavior was observed, probably due to utilizing a flow injection mode of analysis.

Of the tested elements Mn (II), Cr(III) and Mo(VI) did not cause notable interference in either medium at the given concentrations. The negative effect of transition metals was more pronounced for Se(IV) in the presence of 0.06 mol L^{-1} sodium hydroxide than for Se(VI) in deionized water. A possible explanation lies in the formation of precipitates as Zn(II), Fe(III), Ni(II) and Cu(II) are capable of forming poorly soluble compounds with NaOH [46]. These precipitates may adsorb either the analytes or the reaction intermediates; the adsorption of selenite is known for ferric oxyhydroxides [47]. Nevertheless, it is likely that during analysis of real samples these elements were retained in the precipitate during filtering and therefore did not interfere in the determination of Se. Unlike the extracts of the real samples the solutions used in the interference study were not filtered. The small amount precipitate which formed in some cases has been left to settle on the bottom of the volumetric flask and the analysis was carried out on the solution above it. Although the spiking of samples proved that Se is not adsorbed on the matrix, we cannot rule out that possibility if Se is in contact with the interferent for longer time than 30 min. Ca(II) and Mg (II) decreased the repeatability of analytical signals without species and pH preference and Mg(II) increased the signal for Se(IV). This finding is noteworthy as these elements are abundant in dietary supplement samples. On the contrary, presence of Sb(III), As(III) and Te(IV) affected Se(VI) more than Se(IV). In spite of expecting decreased analytical signals due to competition with the other hydride forming elements, the presence of Te(IV) led to 40% increase of Se(VI) response.

Table 3
Determination of Se content in samples of dietary supplements.

Sample	Standard addition method, μg	External calibration method, μg	MW digestion ETAAS, μg	Declared content, μg
A[a]	51 ± 4	52 ± 3	49 ± 4	50
B[b]	36 ± 2	34 ± 3	33 ± 4	30
C[b]	61 ± 9	59 ± 6	51 ± 3	55
D[a]	57 ± 2	55 ± 2	53 ± 5	55
E[b]	22 ± 5	24 ± 2	26 ± 6	25

For detailed information see Section 2.6.
[a] Samples contained sodium selenite and were extracted using NaOH.
[b] Samples contained sodium selenate and were extracted using deionized water.

Table 4
Influence of the selected possible interferents on the recovery of 150 ng mL^{-1} of Se(IV) and Se(VI).

	Interferent concentration	Se(IV) recovery (%) [a]	Se(VI) recovery (%) [b]
Mn(II)	4 mg L^{-1}	97 ± 1	98 ± 3
Zn(II)	1 mg L^{-1}	77 ± 2	97 ± 2
	10 mg L^{-1}	74 ± 6	95 ± 5
Fe(III)	15 mg L^{-1}	85 ± 1	100 ± 4
Cu(II)	500 μg L^{-1}	60 ± 4	93 ± 5
Cr(III)	100 μg L^{-1}	93 ± 5	103 ± 5
Mo(VI)	50 μg L^{-1}	100 ± 2	109 ± 5
I(-I)	150 μg L^{-1}	105 ± 4	105 ± 9
Mg(II)	100 mg L^{-1}	139 ± 9	112 ± 10
Ca(II)	100 mg L^{-1}	103 ± 2	110 ± 3
	200 mg L^{-1}	113 ± 15	115 ± 19
Sb(III)	100 μg L^{-1}	96 ± 6	95 ± 5
	5 mg L^{-1}	86 ± 10	64 ± 8
As(III)	100 μg L^{-1}	94 ± 3	94 ± 2
	5 mg L^{-1}	107 ± 2	78 ± 4
Te(IV)	500 μg L^{-1}	100 ± 2	139 ± 1
	5 mg L^{-1}	98 ± 1	141 ± 1
Ni(II)	5 mg L^{-1}	75 ± 1	101 ± 3
	10 mg L^{-1}	72 ± 1	97 ± 1

$n = 3$.
[a] Determined in 0.06 mol L^{-1} NaOH solution.
[b] Determined in deionized water.

4. Conclusions

A photocatalyst mediated UV-photochemical generation of volatile Se species was successfully demonstrated for the determination of selenite and selenate content in five samples of dietary supplements. Diluted acetic acid was used in combination with TiO_2 as a generation medium. The limits of detection of the method were 0.89 ng mL^{-1} and 0.68 ng mL^{-1} for selenite and selenate, respectively. In determining the total Se content the method was found comparable to using wet microwave digestion and ETAAS determination of Se, while using much simpler procedure. The method proposed in our work is environmentally friendly and permits an easy implementation of automation due to being based on flow injection set-up. Large standard deviations were observed in both the proposed method and ETAAS, which we attributed to the variability of matrix and Se content between the samples.

Acknowledgements

The work was supported by the Charles University (Project SVV260440 and Project GA UK No. 228214). The authors would also like to thank to Jiří Dědina from the Czech Academy of Science for valuable comments.

Appendix A. Supplementary data

Supplementary data to this article can be found online at http://dx.doi.org/10.1016/j.sab.2017.06.007.

References

[1] B. Markert, S. Fränzle, S. Wünschmann, Chemical Evolution - The Biological System of the Elements, Springer, 2015http://dx.doi.org/10.1007/978-3-319-14355-2.
[2] M.P. Rayman, Selenium and human health, Lancet 379 (2012) 1256–1268, http://dx.doi.org/10.1016/S0140-6736(11)61452-9.
[3] M.P. Rayman, Food-chain selenium and human health: emphasis on intake, Br. J. Nutr. 100 (2008) 254–268, http://dx.doi.org/10.1017/S0007114508939830.
[4] M.P. Rayman, The importance of selenium to human health, Lancet 356 (2000) 233–241, http://dx.doi.org/10.1016/S0140-6736(00)02490-9.
[5] L.V. Papp, J. Lu, A. Holmgren, K.K. Khanna, From selenium to selenoproteins: synthesis, identity, and their role in human health, Antioxid. Redox Signal. 9 (2007) 775–806, http://dx.doi.org/10.1089/ars.2007.1528.
[6] M. Navarro-Alarcon, C. Cabrera-Vique, Selenium in food and the human body: a review, Sci. Total Environ. 400 (2008) 115–141, http://dx.doi.org/10.1016/j.scitotenv.2008.06.024.
[7] H. Steinbrenner, B. Speckmann, A. Pinto, H. Sies, High selenium intake and increased diabetes risk: experimental evidence for interplay between selenium and carbohydrate metabolism, J. Clin. Biochem. Nutr. 48 (2010) 40–45, http://dx.doi.org/10.3164/jcbn.11-002FR.
[8] C. B'Hymer, J.A. Caruso, Evaluation of yeast-based selenium food supplements using high-performance liquid chromatography and inductively coupled plasma mass spectrometry, J. Anal. At. Spectrom. 15 (2000) 1531–1539, http://dx.doi.org/10.1039/b006437h.
[9] G. Vale, A. Rodrigues, A. Rocha, R. Rial, A.M. Mota, M.L. Goncalves, L.P. Fonseca, J.L. Capelo, Ultrasonic assisted enzymatic digestion (USAED) coupled with high performance liquid chromatography and electrothermal atomic absorption spectrometry as a powerful tool for total selenium and selenium species control in Se-enriched food supplements, Food Chem. 121 (2010) 268–274, http://dx.doi.org/10.1016/j.foodchem.2009.11.084.
[10] V. Stibilj, P. Smrkolj, A. Krbavčič, Investigation of the declared value of selenium in food supplements by HG-AFS, Microchim. Acta 150 (2005) 323–327, http://dx.doi.org/10.1007/s00604-005-0335-6.
[11] A. Tyburska, K. Jankowski, Determination of selenium in dietary supplements by optical emission spectrometry after alkaline dissolution and subsequent headspace solid phase microextraction, J. Pharm. Biomed. Anal. 74 (2013) 268–272, http://dx.doi.org/10.1016/j.jpba.2012.11.011.
[12] L. Kozak, M. Rudnicka, P. Niedzielski, Determination of inorganic selenium species in dietary supplements by hyphenated analytical system HPLC-HG-AAS, Food Anal. Methods 5 (2012) 1237–1243, http://dx.doi.org/10.1007/s12161-012-9365-y.
[13] P. Niedzielski, M. Rudnicka, M. Wachelka, L. Kozak, M. Rzany, M. Wozniak, Z. Kaskow, Selenium species in selenium fortified dietary supplements, Food Chem. 190 (2016) 454–459, http://dx.doi.org/10.1016/j.foodchem.2015.05.125.
[14] E. Dumont, K. De Cremer, M. Van Hulle, C.C. Chery, F. Vanhaecke, R. Cornelis, Separation and detection of Se-compounds by ion pairing liquid chromatography-microwave assisted hydride generation-atomic fluorescence spectrometry, J. Anal. At. Spectrom. 19 (2004) 167–171, http://dx.doi.org/10.1039/b307316e.
[15] P. Viñas, I. López-García, B. Merino-Meroño, N. Campillo, M. Hernández-Córdoba, Determination of selenium species in infant formulas and dietetic supplements using liquid chromatography-hydride generation atomic fluorescence spectrometry, Anal. Chim. Acta 535 (2005) 49–56, http://dx.doi.org/10.1016/j.aca.2004.11.068.
[16] F. Gosetti, P. Frascarolo, S. Polati, C. Medana, V. Gianotti, P. Palma, R. Aigotti, C. Baiocchi, M.C. Gennaro, Speciation of selenium in diet supplements by HPLC-MS/MS methods, Food Chem. 105 (2007) 1738–1747, http://dx.doi.org/10.1016/j.foodchem.2007.04.072.
[17] Y.-J. Hsieh, S.-J. Jiang, Determination of selenium compounds in food supplements using reversed-phase liquid chromatography–inductively coupled plasma mass spectrometry, Microchem. J. 110 (2013) 1–7, http://dx.doi.org/10.1016/j.microc.2013.01.009.
[18] J. Zembrzuska, H. Matusiewicz, H. Polkowska-Motrenko, E. Chajduk, Simultaneous quantitation and identification of organic and inorganic selenium in diet supplements by liquid chromatography with tandem mass spectrometry, Food Chem. 142 (2014) 178–187, http://dx.doi.org/10.1016/j.foodchem.2013.05.004.
[19] H. Goenaga Infante, G. O'Connor, Ma. Rayman, R. Wahlen, J. Entwisle, P. Norris, R. Hearn, T. Catterick, Selenium speciation analysis of selenium-enriched supplements by HPLC with ultrasonic nebulisation of ICP-MS and electrospray MS/MS detection, J. Anal. At. Spectrom. 19 (2004) 1529–1538, http://dx.doi.org/10.1039/b411270a.
[20] L. Valiente, M. Piccinna, E. Romero Ale, A. Grillo, P. Smichowski, Determination of selenium in dietary supplements by ETAAS and HG-AAS: a comparative study, At. Spectrosc. 23 (2002) 129–134.
[21] L. Gámiz-Gracia, M.D. Luque De Castro, Determination of selenium in nutritional supplements and shampoos by flow injection-hydride generation-atomic fluorescence spectrometry, Talanta 50 (1999) 875–880, http://dx.doi.org/10.1016/S0039-9140(99)00171-X.
[22] X. Guo, R.E. Sturgeon, Z. Mester, G.J. Gardner, UV vapor generation for determination of selenium by heated quartz tube atomic absorption spectrometry, Anal. Chem. 75 (2003) 2092–2099, http://dx.doi.org/10.1021/ac020695h.
[23] X. Guo, R.E. Sturgeon, Z. Mester, G.J. Gardner, Photochemical alkylation of inorganic selenium in the presence of low molecular weight organic acids, Environ. Sci. Technol. 37 (2003) 5645–5650, http://dx.doi.org/10.1021/es034418j.
[24] X. Guo, R.E. Sturgeon, Z. Mester, G.J. Gardner, UV light-mediated alkylation of inorganic selenium, Appl. Organomet. Chem. 17 (2003) 575–579, http://dx.doi.org/10.1002/aoc.473.
[25] Y. Yin, J. Liu, G. Jiang, Photo-induced chemical-vapor generation for sample introduction in atomic spectrometry, TrAC Trends Anal. Chem. 30 (2011) 1672–1684, http://dx.doi.org/10.1016/j.trac.2011.04.021.
[26] Y. He, X. Hou, C. Zheng, R.E. Sturgeon, Critical evaluation of the application of photochemical vapor generation in analytical atomic spectrometry, Anal. Bioanal. Chem. 388 (2007) 769–774, http://dx.doi.org/10.1007/s00216-006-1044-7.
[27] V.N.H. Nguyen, D. Beydoun, R. Amal, Photocatalytic reduction of selenite and selenate using TiO2 photocatalyst, J. Photochem. Photobiol. A Chem. 171 (2005) 113–120, http://dx.doi.org/10.1016/j.jphotochem.2004.09.015.
[28] E. Kikuchi, H. Sakamoto, Kinetics of the reduction reaction of selenate ions by TiO2 photocatalyst, J. Electrochem. Soc. 147 (2000) 4589–4593, http://dx.doi.org/10.1149/1.1394106.
[29] T.T.Y. Tan, D. Beydoun, R. Amal, Photocatalytic reduction of Se (VI) in aqueous solutions in UV/TiO2 system: kinetic modeling and reaction mechanism, J. Phys. Chem. B 107 (2003) 4296–4303, http://dx.doi.org/10.1021/jp026149+.
[30] T. Tan, D. Beydoun, R. Amal, Effects of organic hole scavengers on the photocatalytic reduction of selenium anions, J. Photochem. Photobiol. A Chem. 159 (2003) 273–280, http://dx.doi.org/10.1016/S1010-6030(03)00171-0.
[31] T. Suzuki, R.E. Sturgeon, C. Zheng, A. Hioki, T. Nakazato, H. Tao, Influence of speciation on the response from selenium to UV-photochemical vapor generation, Anal. Sci. 28 (2012) 807–811, http://dx.doi.org/10.2116/analsci.28.807.
[32] M. Garcıá, R. Figueroa, I. Lavilla, C. Bendicho, On-line photoassisted vapour generation implemented in an automated flow-injection/stopped-flow manifold coupled to an atomic detector for determination of selenium, J. Anal. At. Spectrom. 21 (2006) 582–587, http://dx.doi.org/10.1039/b601650b.
[33] R. Figueroa, M. García, I. Lavilla, C. Bendicho, Photoassisted vapor generation in the presence of organic acids for ultrasensitive determination of Se by electrothermal-atomic absorption spectrometry following headspace single-drop microextraction, Spectrochim. Acta B At. Spectrosc. 60 (2005) 1556–1563, http://dx.doi.org/10.1016/j.sab.2005.10.009.
[34] C. Zheng, L. Yang, R.E. Sturgeon, X. Hou, UV photochemical vapor generation sample introduction for determination of Ni, Fe , and Se in biological tissue by isotope dilution ICPMS, Anal. Chem. 82 (2010) 3899–3904, http://dx.doi.org/10.1021/ac1004376.
[35] M. Rybínová, V. Červený, J. Hraníček, P. Rychlovský, UV-photochemical vapor generation with quartz furnace atomic absorption spectrometry for simple and sensitive determination of selenium in dietary supplements, Microchem. J. 124 (2016) 584–593, http://dx.doi.org/10.1016/j.microc.2015.10.004.
[36] Q. Wang, J. Liang, J. Qiu, B. Huang, Online pre-reduction of selenium(VI) with a newly designed UV/TiO2 photocatalysis reduction device, J. Anal. At. Spectrom. 19 (2004) 715–716, http://dx.doi.org/10.1039/b403129f.
[37] Y.C. Sun, Y.C. Chang, C.K. Su, On-line HPLC-UV/Nano-TiO2-ICPMS system for the determination of inorganic selenium species, Anal. Chem. 78 (2006) 2640–2645, http://dx.doi.org/10.1021/ac051899b.
[38] H. Li, Y. Luo, Z. Li, L. Yang, Q. Wang, Nanosemiconductor-based photocatalytic vapor generation systems for subsequent selenium determination and speciation with atomic fluorescence spectrometry and inductively coupled plasma mass spectrometry, Anal. Chem. 84 (2012) 2974–2981, http://dx.doi.org/10.1021/ac3001995.
[39] W. Yang, Y. Gao, L. Wu, X. Hou, C. Zheng, X. Zhu, Preconcentration and in-situ photoreduction of trace selenium using TiO2 nanoparticles, followed by its determination by slurry photochemical vapor generation atomic fluorescence spectrometry,

Microchim. Acta 181 (2014) 197–204, http://dx.doi.org/10.1007/s00604-013-1101-9.
[40] C. Zheng, L. Wu, Q. Ma, Y. Lv, X. Hou, Temperature and nano-TiO2 controlled photochemical vapor generation for inorganic selenium speciation analysis by AFS or ICP-MS without chromatographic separation, J. Anal. At. Spectrom. 23 (2008) 514–520, http://dx.doi.org/10.1039/b713651j.
[41] B. Campanella, A. Menciassi, M. Onor, C. Ferrari, E. Bramanti, A. D'Ulivo, Studies on photochemical vapor generation of selenium with germicidal low power ultraviolet mercury lamp, Spectrochim. Acta B At. Spectrosc. 126 (2016) 11–16, http://dx.doi.org/10.1016/j.sab.2016.10.007.
[42] J. Dědina, B. Welz, Quartz tube atomizers for hydride generation atomic absorption spectrometry: mechanism for atomization of arsine, J. Anal. At. Spectrom. 7 (1992) 307–314, http://dx.doi.org/10.1039/JA9920700307.
[43] J.M. Marchante-Gayón, C. Thomas, I. Feldmann, N. Jakubowski, Comparison of different nebulisers and chromatographic techniques for the speciation of selenium in nutritional commercial supplements by hexapole collision and reaction cell ICP-MS, J. Anal. At. Spectrom. 15 (2000) 1093–1102, http://dx.doi.org/10.1039/b002372h.
[44] H. Stosnach, Analytical determination of selenium in medical samples, staple food and dietary supplements by means of total reflection X-ray fluorescence spectroscopy, Spectrochim. Acta B At. Spectrosc. 65 (2010) 859–863, http://dx.doi.org/10.1016/j.sab.2010.07.001.
[45] L.S. Balistrieri, T. Chao, Adsorption of selenium by amorphous iron oxyhydroxide and manganese dioxide, Geochim. Cosmochim. Acta 54 (1990) 739–751, http://dx.doi.org/10.1016/0016-7037(90)90369-V.
[46] H. Remy, Lehrbuch der anorganischen Chemie, Bd. 2, Akademische Verlagsgesellschaft Geest & Portig K.-G., Leipzig, 1973.
[47] S. Tam, A. Chow, D. Hadley, Effects of organic component on the immobilization of selenium on iron oxyhydroxide, Sci. Total Environ. 164 (1995) 1–7, http://dx.doi.org/10.1016/0048-9697(95)04423-X.

Comparison of interference in chemical, electrochemical and UV-photochemical vapor generation methods

E. Nováková, M. Rybínová, J. Hraníček, P. Rychlovský, V. Červený

Charles University, Faculty of Science, Department of Analytical Chemistry, Albertov 6, Prague 2, CZ 128 43, Czech Republic, corresponding author: eliska.novakova@natur.cuni.cz

Abstract

This paper deals with the comparison of liquid and gaseous interferences from hydride forming elements, transition metals and electrolytes in chemical, electrochemical and UV-photochemical vapor generation with quartz furnace atomic absorption spectrometric detection. The dependences of the Se atomic absorption signal on increasing concentration of selected interferents are discussed. The similarities and differences between the techniques are compared for individual interferents. The observations made are meant to help analytical chemists determining Se to choose the method of vapor generation most suitable for their matrix. The possibility that Co(II), Cr(III) and Ni(II) could be used to increase the response in UV-photochemical generation of Se volatile species is discussed. It was found that Ni(II) facilitates increased Se signals even in gaseous phase. In general, increased Se signals resulting from modified reactions were associated with the alternative vapor generation methods. Electrochemical vapor generation suffers from permanent interference effects located on the cathode, but these were not observed with chemical and UV-photochemical vapor generation. Among hydride forming elements Sb(III) generally caused more severe effect on the determination of Se than As(III) and the same observation was made with all three methods.

Keywords: interference, selenium, chemical vapor generation, electrochemical vapor generation, UV-photochemical vapor generation

1. Introduction

Volatile species generation permits the separation of the determined element from the sample matrix thus reducing spectral interference. However, this advantage is often offset by the effects caused by the matrix during the generation process (liquid phase interference) and during the transport of the volatile species and the atomization process (gaseous phase interference). Liquid phase interference is usually caused by reduced generation efficiency due to either competition with other hydride forming elements or by decomposition of the evolved hydrides on solid particles formed in the reaction medium.[1] Gaseous phase interference is typical for other hydride forming elements. [2] It can be decreased by the choice of atomizer as it is related to the atomization mechanism in quartz furnace or miniature diffusion flame atomizers. [3–5]

Selenite can be converted to a volatile compound and subsequently determined using chemical generation of volatile species using tetrahydroborate (CVG) [6] or alkylation with tetraethylborate or tetrapropylborate [7,8]. It can also be determined using electrochemical generation of volatile species (EcVG) [9] and ultraviolet photochemical generation of volatile species (UV-PVG) [10].

In CVG the most attention has been given to liquid interference caused by the transition and noble metals. The mechanism is attributed to the adsorption or decomposition of the evolved hydride on reduced metal or metal-boride

particles. [1] The origins of this conclusion started with Kirkbright and Tadia who observed the formation of a fine black precipitate during the chemical generation of AsH_3 in the presence of copper, nickel, platinum and palladium and associated it with the decrease of signals. [11] Since then other works were published dealing with the topic. [12–15] Henden et al. [16] proposed that the species of As and Sb adsorbed on Ni borides may not be the generated hydrides but rather the dissolved species of As(III), As(V) and Sb(III). They also attempted to characterize the nickel-boride particles concluding that the nanoparticles produced at their reaction conditions had amorphous structure with diameter of less than 40 nm and contained Ni, Ni_2B, Ni_3B and $Ni(OH)_2$.

The need for more environmentally friendly and robust analytical methods led researchers to developing alternative methods of volatile species generation aiming at lower limits of detection and better tolerance to the presence of concomitants. EcVG is a substantial cost-effective alternative to chemical volatile species generation using $NaBH_4$. Laborda et al. summarized in their review the bulk of knowledge of the EcVG technique and showed that its performance is comparable with CVG. [17] Liquid interferences in EcVG result from processes taking place on the cathode. The most important mechanism of interference appears to be reduction of transition metals on the cathode surface causing a change in the generation efficiency. [18] Also while metal-boride interferences do not exist in this generation method a possible interaction of the generated hydride with reduced metal particles released from the cathode cannot be ruled out.

UV-Photochemical generation of selenium volatile species was pioneered in 2003 by Guo et al. [10,19,20]. The generation process is based on UV irradiation of sample in the presence of low molecular weight organic acid. Compared to the previous techniques, almost no hydrogen is formed during the generation process and it has to be added if it is required for atomization. [10] First papers dealing with UV-PVG published a good tolerance of the technique to the presence of interferents and the tolerance was explained by the low reduction efficiency of the radical intermediates, which were assumed to be responsible for the formation of volatile compound. [10] Nevertheless, the definite mechanism of formation of the volatile compound remains a matter of discussion. [21]

This work compares the interferences in three volatile species generation methods to uncover similarities in location and mechanism of interferences. We also highlight possible ways to increase the sensitivity of Se determination by UV-photochemical generation using reaction modifiers. Some general trends have been observed, which might even be applicable to other hydride forming elements than selenium.

2. Experimental

2.1. Reagents

Deionized water prepared by the MilliQplus system (Millipore, USA) was used throughout the measurements. If not stated otherwise all chemicals were of analytical purity. Selenium samples were diluted from a stock solution (1000 $\mu g\ mL^{-1}$ of Se) prepared from sodium selenite pentahydrate (Sigma-Aldrich, USA). Hydrochloric acid (suprapure grade, Merck, Germany) diluted to 1.0 $mol\ L^{-1}$ served as the catholyte solution and 2.0 $mol\ L^{-1}$ sulphuric acid (research grade, Merck, Germany) as the anolyte solution in the EcVG of selenium hydride. Formic acid diluted to 0.5 $mol\ L^{-1}$ was used as photochemical reagent in UV-PVG and 1.0 $mol\ L^{-1}$ HCl and 0.5% $NaBH_4$ in 0.4% NaOH were used in the chemical vapor generation. Argon of the 99.998 % purity (Linde, Czech Republic) was always used

as the carrier gas. Hydrogen of 99.90 % purity was used as an auxiliary atomization gas in UV-PVG of selenium volatile species.

The effect of concomitant ions on the selenium volatile species generation was evaluated using the solutions diluted from standard solutions of As, Sb, Pb, Cd, Ni, Fe, Mn, Co, Cr, Cu, Ag (prepared in HNO_3, all from Analytika, Czech Republic). Pure mineral acids were used to prepare the diluted solutions of HNO_3 (extrapure grade, Merck, Germany), H_2SO_4 (Merck, Germany), HCl (suprapure grade, Merck, Germany), H_3PO_4 (Merck, Germany). The solutions of the respective salts of the above mentioned acids were prepared from $NaNO_3$, Na_2SO_4, Na_3PO_4 (all from Lachner, Czech Republic) and NaCl (Merck, Germany).

2.2. Instrumentation

The measurements were carried out using Unicam 939 AA spectrometer (Unicam, UK). The absorption of radiation was detected at the wavelength of 196.0 nm using a band-pass of 0.5 nm. An externally heated quartz furnace atomizer (RMI, Czech Republic) was used for the atomization of the generated Se volatile species at 950 °C. A reaction coil made of 0.8 m (1.0 mm i.d./ 2.0 mm o.d.) of PTFE tubing (Sigma-Aldrich, USA) was used in CVG. A length of 3.5 m (1.0 mm i.d./1.4 mm o.d) PTFE tubing coiled around a 20W low pressure Hg lamp (Ushio, Japan) was used as a reactor in UV-PVG. The photochemical reactor is described in detail in previous publications [22,23]. Thin-layer flow-through electrochemical cell with lead wire cathode (Sigma-Aldrich, USA) and Pt foil anode (Goodfellow, UK) described in [24] was used in EcVG. Cathodes were changed after every interferent. A MasterFlex L/S peristaltic pump (Cole-Parmer, USA) was used for driving the solutions. Mass flow controllers (Cole-Parmer, USA) for flow rates 0-50 mL min^{-1} and 0-100 mL min^{-1} were used for the control of the flow rates of Ar and H_2 gasses. The experimental setup including the three reactors is shown in Fig.1.

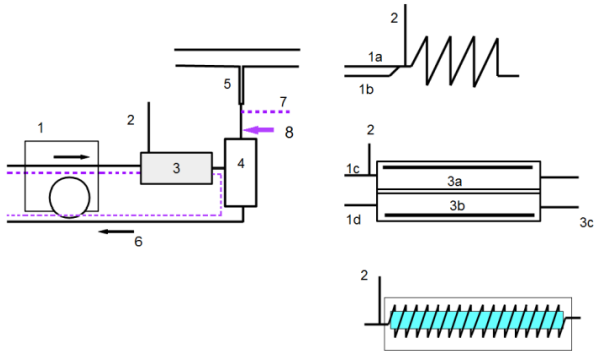

Fig.1: Experimental setup and reactors, 1 – peristaltic pump, 2 – carrier gas (Ar), 3 – reactor (A – CVG, B – EcVG, C – UV-PVG), 4 – gas / liquid phase separator, 5 – heated quartz furnace atomizer, 6 – waste, 1a – HCl and sample channel, 1b – $NaBH_4$ channel, 1c – catholyte and sample channel, 1d – anolyte channel, corresponds to dashed purple line in set-up, 3a – cathode compartment, 3b – anode compartment, 3c – anolyte output, 7 – atomization gas (H_2, UV-PVG only), 8 – connection of channels during separate generation of analyte and interferent

2.3. Measurement procedure and evaluation of results

The quantification of the liquid phase interference was carried out by addition of the respective interferent into the Se sample. The attained signal was then compared to the signal of the same concentration of selenium without interferent. Interferent effects were measured in series of increasing concentrations of a given concomitant element. Each series was preceded by a repeated measurement of Se sample without any interferent added and the mean absorbance of that sample was taken as reference. Measured absorbance in the presence of concomitants (A_{sample}) was divided by the absorbance of pure Se solution (A_{Se}) and expressed as relative Se response (RSR) in per cent units; see equation 1. Selenium solutions without interferent were randomly inserted into the measurement sequence to show possible memory effects.

$$RSR = A_{sample} / A_{Se} \cdot 100\ [\%] \quad (1)$$

Experiments employing separate generation of volatile compounds of As, Sb, Pb and possible volatile forms of Ni, Cu were carried out to classify the mechanism of interference. In these series of experiments, the volatile form of the interferent was generated in one channel and Se volatile species in the second channel and these channels were connected after phase separation and prior to the introduction into the atomizer. Pairs of generators and phase separators of the same design and dimensions were used. Experimental conditions were selected to keep the atomization conditions unchanged. All conditions were the same as the optimum conditions only the gas flow rate was halved in each of the channels.

Due to different Se concentrations used with different volatile species generation methods (see section 3.1), the dependence of relative Se response was plotted against the ratio of concomitant -to-Se mass concentrations rather than directly against the concentrations of concomitants.

3. Results and discussion

3.1. Optimized experimental conditions and figures of merit

Experimental conditions were optimized for each generation approach prior to the interference study, but the optimization experiments are not discussed here. The obtained optimized conditions for CVG were 1.0 mol L^{-1} HCl; 0.5% $NaBH_4$ in 0.4 % NaOH, flow rate of HCl / sample 5.0 mL min^{-1}, reducing agent flow rate 1.7 mL min^{-1}, carrier gas flow rate 20 mL min^{-1}. The optimized conditions for EcVG were 1.0 mol L^{-1} HCl serving as catholyte and 2.0 mol L^{-1} H_2SO_4 as anolyte, generation current 1.0 A on the cathode, catholyte / sample flow rate 5.5 mL min^{-1} and anolyte flow rate 2.0 mL min^{-1}, carrier gas flow rate 70 mL min^{-1}. Similarly, for UV-PVG the conditions were 0.5 mol L^{-1} formic acid, formic acid / sample flow rate 6.0 mL min^{-1}, carrier gas flow rate 15 mL min^{-1} and H_2 flow rate 2 mL min^{-1}. Using the apparatus and experimental conditions described in experimental section we achieved LODs 58 pg mL^{-1}, 490 pg mL^{-1}, 45 pg mL^{-1} for CVG, EcVG and UV-PVG with LDRs reaching up to 15.0, 100.0, 12.0 ng mL^{-1}, respectively. The attained sensitivities were 0.0408, 0.00758, 0.0327 mL pg^{-1} and repeatabilities calculated as relative standard deviations for concentration from the middle of the calibration curve were 1.40 %, 3.10 %, 1.50 %, respectively. The higher LOD achieved with EcVG could be explained by higher noise associated with the deterioration of the cathode surface due to longer use. Due to the fact that we did not achieve similar LODs in all

tested methods we chose the concentration of selenium giving the absorbance of approximately 0.20 for the interference study; the concentrations of Se used were 5 ng mL^{-1} in CVG and UV-PVG and 25 ng mL^{-1} in EcVG.

3.2. Visual observations during the interference study

No formation of visible reduced metal layer was observed with UV-PVG and CVG and measurements of sample without interferent at random intervals did not attest to notable memory effects caused by the studied interferents. On the other hand, in EcVG signals for samples without interferent randomly inserted into the series gradually changed suggesting permanent memory effects. This observation is consistent with our previous studies. [25] After the addition of copper a change of color of the cathode surface was observed. This is in accordance with the theory of the modification of the cathode surface. [26]

3.3. Liquid interference

3.3.1. CVG

3.3.1.1. Hydride forming elements

Cross-influence of the hydride forming elements in volatile species generation has been discussed by other authors [27–30], therefore, we restrict ourselves to the quantification and comparison of the effects of As (III), Sb (III), Pb (II) and Cd (II) we observed in this work. We measured unaffected signals in the presence of Sb (III) up to the concentration 100 ng mL^{-1} but the RSR at 500 ng mL^{-1} of Sb (III) was only 13 %. In the case of As (III), good tolerance was observed in the presence of 20 ng mL^{-1}, but 500 ng mL^{-1} of As (III) gave response 22 %. See Fig.2 for the dependence of interference on growing content of As and Sb. On the other hand, we did not observe any interference in the presence of Pb (II) in the samples even at concentrations as high as 100 µg mL^{-1}. Cd (II) has demonstrated similar behavior to lead but interference effects appeared at 20 µg mL^{-1}. Signals fell to only 15 % for 100 µg mL^{-1} of Cd (II) making it a more important interferent than Pb (II). The low effect of Pb (II) could be explained by the fact that successful chemical generation of its volatile species requires the addition of reaction modifiers. [31,32]

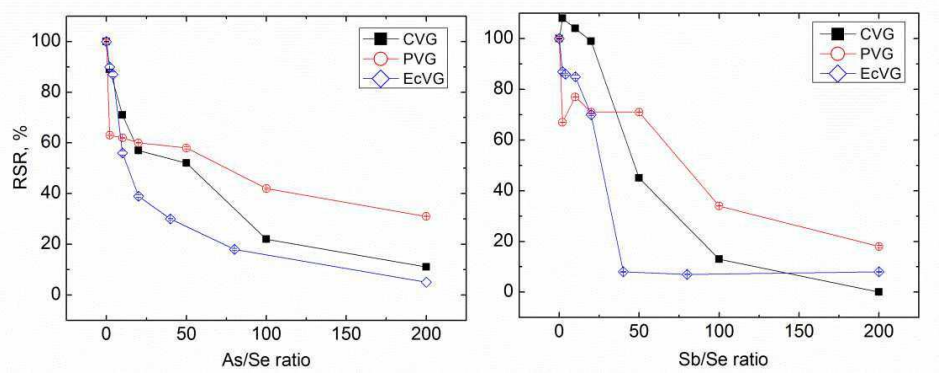

Fig.2: Effect of As and Sb in liquid phase on CVG, EcVG and UV-PVG, results expressed as relative selenium response (%), amount of interferent expressed as concomitant-to-Se mass concentration ratio, see section 2.3 for further explanation of axes labels

3.3.1.2. Ions of transition and noble metals

Transition metals (mainly Cu, Ni) are considered important interferents in CVG. We observed varied effects, although when a pronounced effect appeared, it was always negative. The most notable interference was observed with Cu (II), Ni (II) and Ag (I) with silver being the most severe interferent. Pagliano et al. published that the presence of noble metals (Au, Pd and Pt) can affect the hydride generation through modification of hydrogen transfer from $NaBH_4$ to the analyte element. They termed this transfer of a larger amount of hydrogen derived from the solvent to the final hydride a mechanistic interference. [33] Only 5 ng mL^{-1} of Ag was within the tolerable ±10 % limit. High contents of Cu decreased Se response more than Ni. For example 1000 ng mL^{-1} of Cu (II) gave response of only 2 % while the same concentration of Ni (II) in the sample gave Se response of 83 %. On the other hand, Fe (III), Mn (II) and Cr (III) did not significantly affect the analytical signals even at high surplus of interferent over Se (see Table 1).

Table 1: Effect of hydride forming elements and transition metals in liquid phase on selenium volatile species generation in CVG, EcVG and UV-PVG methods, results expressed as relative selenium response (%), amount of interferent expressed as concomitant-to-Se mass concentration ratio, for details see section 2.3

Concomitant element	concomitant-to-Se ratio	CVG [a]	EcVG [b]	UV-PVG [a]
As (III)	10:1	71	56	62
	100:1	22	n	42
Sb (III)	10:1	104	85	77
	100:1	13	n	34
Pb (II)	10:1	104	79	83
	200:1	101	85	3
Cr (III)	200:1	100	30	113
Mn (II)	10:1	114	84	101
	200:1	106	101	112
Fe (III)	10:1	102	82	65
	200:1	104	97	64
Co (II)	200:1	99	82	188
Ni (III)	10:1	98	87	97
	200:1	83	33	121
Cu (II)	10:1	102	61	132
	200:1	2	176	4
Ag (I)	10:1	52	74	19
	200:1	0	34	0
Cd (II)	100:1	99	n	79
	200:1	105	89	103

[a] 5 µg/L of Se (IV)
[b] 25 µg/L of Se (IV)
n not determined

3.3.1.3. Acids and salts

Compared to alternative volatile compounds generation methods, CVG was found fairly resistant to the presence of inorganic acids. No interference was observed in the presence of 1.0 mol L^{-1} sulphuric acid and phosphoric acid.

Similar behavior was observed for inorganic salts – sulphates and phosphates did not cause interference up to 1.0 mol L^{-1}. Nitric acid was tolerated only to 0.1 mol L^{-1} and presence of 1.0 mol L^{-1} led to the relative Se response of 65 %. The presence of nitrates was tolerated up to the concentration of 0.5 mol L^{-1}. The nitric acid interference is likely due to the diminishment of the selenium form available for generation due to oxidation character of nitric acid. Another possibility is production of nitrogen oxides interfering either in the liquid or in the gaseous phase similar to the presence of nitrites in the solution. [34] The effect of hydrochloric acid was not tested, because it served as reaction medium. Mild concentrations of chloride might act as reaction modifiers as 0.1 mol L^{-1} of NaCl led to obtaining the relative Se response of 123 % and concentration 0.5 mol L^{-1} to 160 %. This observation was surprising, because it contradicts all previous results suggesting that we might have achieved complete conversion of analyte to its volatile compound.

Table 2: Effect of inorganic acids and their sodium salts in liquid phase on selenium volatile species generation in CVG, EcVG and UV-PVG methods, results expressed as relative Se response (%), amount of interferent expressed as electrolyte concentration, for details see section 2.3

Concomitant electrolyte	Electrolyte conc., $\cdot 10^{-3}$ mol L^{-1}	CVG [a]	EcVG [b]	UV-PVG [a]
H_2SO_4	5	95	104	91
	50	101	99	38
	250	105	86	7
Na_2SO_4	5	91	100	89
	50	108	85	96
	250	95	72	104
HCl	5	n	n	153
	100	n	n	104
	500	n	n	10
NaCl	10	98	78	105
	50	104	49	91
	250	144	27	45
	500	160	9	n
HNO_3	5	107	96	230
	50	106	9	6
	1000	65	n	n
$NaNO_3$	5	94	111	146
	50	92	12	3
	500	92	n	n
H_3PO_4	5	109	76	101
	100	103	52	77
	1000	101	13	70
Na_3PO_4	5	121	106	88
	50	120	117	98
	250	n	45	n

[a] 5 µg/L of Se (IV)
[b] 25 µg/L of Se (IV)
n not determined

3.3.2. EcVG

3.3.2.1. Hydride forming elements

We observed results contrary to works proposing that EcVG is less liable to interference from other hydride forming elements than CVG. In general, when As or Sb were added into the liquid phase we observed very similar dependences of the relative Se response to those observed in CVG. Low concentrations of Sb led to more interference than respective concentrations of As. Pb (II) exhibited only small interference up to 10 μg mL^{-1}, but presence of higher concentrations led to steep fall of signals, perhaps due to a large surplus of lead over selenium in the vicinity of the cathode. Separate generation of lead volatile compound showed that interference of Pb may be at least partially attributed to atomization interferences (see Section 3.4.2.). Cd again showed similar behavior to Pb, but unlike in CVG Pb interfered more than Cd possibly because Pb (II) is not inert to EcVG. [35] No irreversible memory effects were observed with Cd.

3.3.2.2. Ions of transition and noble metals

Ding and Sturgeon [36] published severe interference (both direct and memory effects) of nickel and copper on the determination of Se. They observed "poisoning" of the Pb cathode in the presence of 7.5 μg mL^{-1} Cu (II). Also presence of 40 μg mL^{-1} of Ni (II) in the solution of 4 ng mL^{-1} selenium led to the decrease of response to 60 % compared to solution without interferent. Laborda et al. concluded that Cu is the source of the most severe interference in EcVG. [17] Conversely, Junková et al. [25] published that Cu led to a less pronounced interference effects in EcVG than in CVG, which was not observed in this study. However the different effects could be explained by the memory effects encountered in our study. These published data led to the expectation of interference effects with similar trends to CVG, because all of them described negative effects. We observed two kinds of dependences with transition metals. Ni, Cr and Ag exhibited only negative influence, but Mn, Fe and Cu exhibited a more complicated behavior. At low concentrations of interferent the Se signals decreased, however in certain concetration regions the observed effect of interferent was positive. From now on, these effects will be termed reaction modification instead of interference. Cu and Mn exhibited an increase in Se signal in the 1-10 μg mL^{-1} concentration range, Fe in 1-5 μg mL^{-1} and Co in 2-5 μg mL^{-1} range. The presence of 2 μg mL^{-1} of Cu (II) actually led to the response of 216 %. Similar observations regarding the effect of Cu were also made for the vapor generation of other elements. Pohl et al.[37] published increased As signals after addition of 5 μg mL^{-1} Cu to the solution of 2 μg mL^{-1} of As. Arbab-Zavar et al. [38] published 30% rise of Tl signals in the presence of 10 μg mL^{-1} Cu from Pb-Sn cathode. It is an accepted fact that Pb has a very high hydrogen overvoltage and represents one of the cathode materials with the highest generation efficiency.[18] It is safe to assume that the increase of response at higher Mn, Fe and Cu concentrations is not due to increased generation efficiency. We hypothesized one of the following effects: i) desorption of adsorbed Se from the Pb cathode surface caused by surplus of interferent, ii) stabilization of the volatile Se compound in gaseous phase on cogenerated volatile form of interferent. The second assumption was tested experimentally, because reaction modification in the presence of various transition elements were encountered also in UV-PVG. The experiments employed separate generation of volatile Se compound and volatile compounds of selected interferents (As, Sb, Pb, Ni, and Cu) and the results are described in Section 3.4. The results observed with EcVG did not support our hypothesis as stabilization of volatile compound of Se on volatilized forms of Ni and Cu was not observed with this method of generation.

In liquid phase Ag (I) had purely signal-depressing effects but smaller than in CVG or UV-PVG; content of 10 ng mL^{-1} decreased the relative Se response to 84 % and 1 µg mL^{-1} to 59 %. Presence of 100 ng mL^{-1} and 1 µg mL^{-1} of Ni gave responses of 95 % and 66 %, respectively and presence of equal concentrations of Cr (III) suppressed relative responses to 74 % and 51 %, respectively.

The decrease of Se signals with growing concentration of interferent during the measurement sequence is a sum of memory and immediate interference effects. Memory effects caused by permanent alteration of cathode surface were observed with all transition metals with the exception of Fe(III) and Mn(II). Measurement of Se solutions without interferent inserted into the sequence gave approximately the same response as they did at the start of the sequence before the first introduction of ferric or manganous ions. All observed interference effects were due to immediate presence of Fe(III) or Mn(II) in the solution.

3.3.2.3. Acids and salts

One more mechanism of interference of inorganic salts and acids can be expected in EcVG compared to CVG: the formation of insoluble salts on the surface of the lead cathode reducing the generation efficiency. [18] This mechanism was a probable source of the phosphate interference. The addition of phosphoric acid caused decrease of response even in low concentrations and 1.0 mol L^{-1} gave relative Se response of only 13 % and similar, although, less pronounced trend, was observed in the presence of phosphate.

On the other hand, sulphuric acid, which would be expected to act as a strong interferent due to the formation of $Pb(SO_4)_2$, did not decrease the signals in concentrations below 0.1 mol L^{-1} and in the concentration of 1.0 mol L^{-1} led to a relative response of 68 %. Very similar results were obtained with sulphate. Nitric acid in general caused loss of signals, but low concentrations of nitrate (0.002 mol L^{-1}) caused increased relative Se response (up to 159 % compared to 116 % in the acid). Starting with 0.005 mol L^{-1} both interferents strongly suppressed the generation of Se volatile compound. Effect of hydrochloric acid was not studied due to its presence in the reaction medium, but chloride decreased the relative Se response. Deterioration of Pb cathode surface in NaCl due to slow dissolution of Pb facilitated by electric current was observed and published by our group in previous publication.[39]

3.3.3. UV-PVG

3.3.3.1. Hydride forming elements

In general, the observed trends of the effects of As and Sb were very similar to CVG and EcVG. That would not be surprising if the generated volatile species were the same in all generation techniques. The products of Se CVG and EcVG are assumed to be hydrides while the product of the UV-photochemical volatile species generation from formic acid should be the mix of selenium hydride and selenium carbonyl. [10,17,19,40] Nevertheless, the composition of the produced volatile compounds was not tested in this work. Very serious interference has been observed for As (III) and Sb (III) (see Fig 2). It would appear that even trace content of As and Sb can decrease Se signals as relative responses below 80 % of relative selenium absorbance were observed at only 1 ng mL^{-1} As or Sb. However, at the same time the decrease of relative Se response with growing surplus of Sb was less steep than for CVG.

The behavior of Pb (II) and Cd (II) did not resemble that of the typical hydride forming elements. No interference was observed for Pb (II) below 20 ng mL^{-1}, but response corresponding to the presence of 250 ng mL^{-1} (50:1 ratio)

of Pb (II) was only 13 %. The behavior of Cd was closer to the behavior of transition metals and is discussed in section 3.3.3.2.

3.3.3.2. Ions of transition and noble metals

Guo et al [10] published that no interference from Ni or Co on the determination of 100 μg L^{-1} of Se (IV) was detected in the acetic acid medium, even for concentrations as high as 500 mg L^{-1} for Ni (II) and 100 mg L^{-1} for Co (II). On the other hand, only 3 μg mL^{-1} of Fe (II) decreased the response by 20 %. Their results also showed that Fe (II) and Fe (III) could have different effects on the response. We observed in our experiments that an apparent interference or reaction modification depends on the concentration of concomitant as much as on its identity. Using the examples of Co (II) and Ni (II) we observed signals corresponding to the pure sample or higher in the interferent concentration ranges of 50 – 1000 ng mL^{-1} (Co) and 50-10000 ng mL^{-1} (Ni), (see Fig. 3). In the case of Ni the increased values appear to form a wide flat maximum and its addition could be used to increase sensitivity of UV-PVG determination of Se. Some authors possibly noticed the same and recently similar phenomenon has been used for trace metal assisted photochemical generation of Pb and As. [41,42] Very similar effects were observed when volatile compounds of Ni (II) were generated separately and these results are discussed in Section 3.4.3. Slightly increased Se response (up to 20 %) was also observed in the presence of Cr (III) and Mn (II), but their behavior was not studied in detail. Similarly to EcVG we observed different behavior of Cu and Ag. The presence of Ag (I) caused only negative interference effects in the form of sharp decline of signals from 5 ng mL^{-1}. On the other hand, presence of 10 ng mL^{-1} Cu (II) resulted in Se response of 175 % (increase was concentrated to a range of 1-50 ng mL^{-1}, see Fig.3).

Addition of Fe (III) decreased the response by 33 % even when its concentration was 1 ng mL^{-1} and this decrease was constant to 1 μg mL^{-1}. Presence of Cd (II) led to the decrease of response in the region of 10 – 100 ng mL^{-1} but no interference was observed at 500 and 1000 ng mL^{-1}.

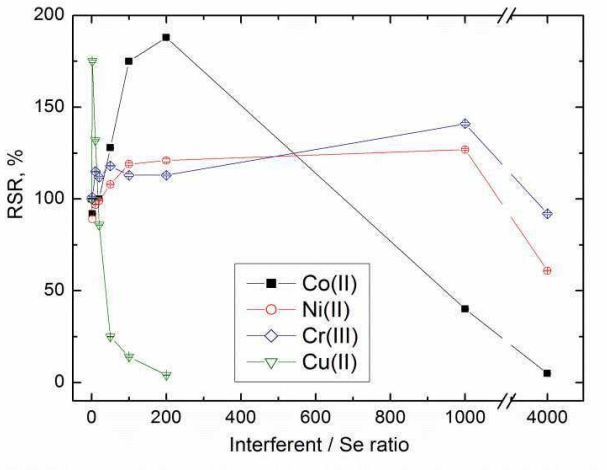

Fig.3: Effect of Co, Ni, Cr and Cu in liquid phase on UV-PVG of Se, results expressed as relative selenium response (%), amount of concomitant expressed as interferent-to-Se mass concentration ratio, see section 2.3 for explanation of axes labels

3.3.3.3. Acids and salts

UV-PVG appears to be the most susceptible to the presence of acids and salts. Previously discussed was mainly the effect associated with the addition of nitric acid. [10,20,23,43] Notable increase of measurement sensitivity was observed when low concentrations of nitric acid were added to formic acid reaction medium. [20] We made the same observation, as 0.005 mol L^{-1} of nitric acid increased the signal more than twice (relative Se response 230 %). However, any further increase of nitric acid concentration led to loss of signal. At 0.05 mol L^{-1} the absorbance reached zero value. [43] This observation means that samples acidified with nitric acid have to be pretreated prior to analysis to reduce the content of nitric acid. Similar observation only less pronounced was made with nitrate. The addition of hydrochloric acid and chloride led to different dependencies. Chloride did not interfere up to 0.02 mol L^{-1} and then decreased with the Se signals reaching zero absorbance at 0.5 mol L^{-1}. Hydrochloric acid caused increase of Se absorbance with maximum 155 % at 0.015 mol L^{-1}. Assuming, that UV radiation causes production of Cl•, we would expect similar trend for HCl and chloride. At the same time, we do not rule out some combined acid-base and redox reactions.

Sulphuric acid was observed to cause interference in concentrations higher than 0.05 mol L^{-1} and relative absorbance dropped to zero at 0.5 mol L^{-1} but sulphate was tolerated up to 0.5 mol L^{-1}. The smallest effect was observed with phosphoric acid and phosphates making UV-PVG a more suitable generation method for samples with phosphate content (e.g. biological) then EcVG.

3.4. Gasseous phase interference study

3.4.1. CVG

More serious interference was observed with Sb than with As in CVG while no interference was observed with Ni, Cu and Pb, when the channels were connected prior to atomization.

3.4.2. EcVG

We observed interference of As and Sb in the gas phase similarly to CVG including more serious interference from Sb than from As. Some atomization interference was also observed in the case of Pb, which is in concordance with the fact that unlike in CVG it is possible to generate volatile compound from Pb (II). [35,44] Slight interference was also observed in the cases of Ni and Cu; the effect could have been caused by volatilized nanoparticles of the reduced metals. The observation also led us to the conclusion that increase of relative Se responses achieved with the addition of Cu (II) into the solution was caused by effects taking place on the cathode.

3.4.3. UV-PVG

Unlike in CVG and EcVG the interference of As and Sb during atomization was negligible and very similar, mild interference was again caused by Pb. Slight interference was also observed in the presence of Cu showing again that the reaction modification leading to increased relative Se responses is likely limited to liquid phase. Though the results are not conclusive due to a very narrow range in which the effect appeared. Different behavior was observed

with Ni; unlike in CVG or EcVG we observed increased Se signals even when Ni was generated in a separate reactor. A possible explanation may be stabilization of Se on a volatile Ni compound. A determination of Ni at 232.0 nm wavelength via its UV photochemical volatile species generation at the same conditions as Se optimum was attempted with negative results. No Ni signals were observed, but there is still a possibility that the compound cannot be atomized at the given atomization conditions or that it decomposes or adheres to the surfaces before reaching the atomizer. The effect of Ni may be associated with the past use of Ni solution as a modifier in ETAAS determination of Se. [45]

4. Conclusions

All methods of volatile species generation suffer from interferent effects caused by concomitant elements. Choosing an optimum method for the determination of analyte requires also knowledge of the likely concomitants and the severity of their effects for a particular analyte. This paper presents a comparison of interferences in chemical, electrochemical and UV-photochemical volatile species generation of Se divided into categories based on the nature of the concomitant. In general, interferences in EcVG and PVG were found comparable, but in addition EcVG suffered also from memory effects. From these two alternative techniques PVG is the more sensible choice. The best resistance to interference effects from transition metals and electrolytes was observed with CVG. Hydride forming elements caused a decrease of signal regardless of the generation approach and interference from As and Sb in the liquid phase showed similar dependences for all three methods despite the fact that different volatile Se species may have been produced. Separate generation of interferent proved that the interference mechanism for As and Sb lies in the gaseous phase, probably during the atomization step. Observation suggests the same mechanism for Pb at least for EcVG and PVG. No conclusion could be made for CVG because no interference was observed due to the inertness of Pb (II) to the reaction with $NaBH_4$.

Interferent effects from transition metals were more varied. For instance CVG was found relatively immune to the presence of Fe (III) and slightly less to the presence of Ni (II), but the signals dropped in the presence of Cu and Ag. Similarly, the UV-PVG was very sensitive to the presence of Cu and Ag, but wide ranges of Cr, Co and Ni concentrations led to a stable increase of signals and, therefore, these elements could be used as reaction modifiers for improving the sensitivity of Se determination. EcVG was the most immune to the presence of Ag in the solution from the three tested methods. The increased signals in the presence of several transition metals, which acted as reaction modifiers, also show that the generation and transport efficiencies in EcVG and PVG were well below 100 %. Otherwise the increased signals would not have been observed.

Generally, the effects of inorganic acids and their respective salts were similar, however exceptions to this rule were observed in the alternative methods. Namely HCl and chloride behaved differently in UV-PVG and HNO_3 and nitrate in EcVG. From the three tested methods CVG would be the most suitable for analysis of samples with high salt content.

Acknowledgements: This work was financially supported by the Charles University (Projects SVV 260440 and GA UK 228214) and by the Grant Agency of the Czech Republic (project GACR 14-23532).

Conflicts of interest: none.

Statement of Human and Animal Rights: Not applicable, no experiments have been conducted on animals or human subjects.

References:

1 A. R. Kumar and P. Riyazuddin, *TrAC - Trends Anal. Chem.*, 2010, **29**, 166–176.

2 P. Barth, V. Krivan and R. Hausbeck, *Anal. Chim. Acta*, 1992, **263**, 111–118.

3 J. Dědina and T. Matoušek, *J. Anal. At. Spectrom.*, 2000, **15**, 301–304.

4 É. M. de Moraes Flores, A. Medeiros Nunes, V. Luiz Dressler and J. Dědina, *Spectrochim. Acta - Part B At. Spectrosc.*, 2009, **64**, 173–178.

5 J. Dědina, *Spectrochim. Acta - Part B At. Spectrosc.*, 2007, **62**, 846–872.

6 R. E. Sturgeon and Z. Mester, *Appl. Spectrosc.*, 2002, **56**.

7 E. Dimitrakakis, C. Haberhauer-Troyer, Y. Abe, M. Ochsenkühn-Petropoulou and E. Rosenberg, *Anal. Bioanal. Chem.*, 2004, **379**, 842–848.

8 P. Wu, L. He, C. Zheng, X. Hou and R. E. Sturgeon, *J. Anal. At. Spectrom.*, 2010, **25**, 1217–1246.

9 A. Brockmann, C. Nonn and A. Golloch, *J. Anal. At. Spectrom.*, 1993, **8**, 397–401.

10 X. Guo, R. E. Sturgeon, Z. Mester and G. J. Gardner, *Anal. Chem.*, 2003, **75**, 2092–2099.

11 G. F. Kirkbright and M. Taddia, *Anal. Chim. Acta*, 1978, **100**, 145–150.

12 A. B. Welz and M. Melcher, *Analyst*, 1984, **109**, 577–579.

13 B. Welz and M. Melcher, *Analyst*, 1984, **109**, 569–572.

14 D. Bax, J. Agterdenbos, E. Worrell and J. B. Kolmer, *Spectrochim. Acta Part B At. Spectrosc.*, 1988, **43**, 1349–1354.

15 A. D 'ulivo, L. Lampugnani and R. Zamboni, *J. Anal. At. Spectrom.*, 1991, **6**, 565–571.

16 E. Henden, Y. İşlek, M. Kavas, N. Aksuner, O. Yayayürük, T. D. Çiftçi and R. İlktaç, *Spectrochim. Acta Part B At. Spectrosc.*, 2011, **66**, 793–798.

17 F. Laborda, E. Bolea and J. R. Castillo, *Anal. Bioanal. Chem.*, 2007, **388**, 743–751.

18 E. Denkhaus, A. Golloch, X. M. Guo and B. Huang, *J. Anal. At. Spectrom.*, 2001, **16**, 870–878.

19 X. Guo, R. E. Sturgeon, Z. Mester and G. J. Gardner, *Appl. Organomet. Chem.*, 2003, **17**, 575–579.

20 X. Guo, R. E. Sturgeon, Z. Mester and G. J. Gardner, *Environ. Sci. Technol.*, 2003, **37**, 5645–5650.

21 R. E. Sturgeon and P. Grinberg, *J. Anal. At. Spectrom.*, 2012, **27**, 222–231.

22 M. Rybínová, V. Červený, J. Hraníček and P. Rychlovský, *Microchem. J.*, 2016, **124**, 584–593.

23 M. Rybínová, V. Červený and P. Rychlovský, *J. Anal. At. Spectrom.*, 2015, **30**, 1752–1763.

24 J. Šíma, P. Rychlovský and J. Dědina, *Spectrochim. Acta - Part B At. Spectrosc.*, 2004, **59**, 125–133.

25 G. Junková, J. Šíma and P. Rychlovský, *Chem. Pap.*, 2003, **57**, 192–196.

26 E. Bolea, F. Laborda, M. A. Belarra and J. R. Castillo, *Spectrochim. Acta Part B At. Spectrosc.*, 2001, **56**, 2347–2360.

27 A. D'Ulivo and J. Dědina, *Spectrochim. Acta - Part B At. Spectrosc.*, 1996, **51**, 481–498.

28 B. Welz and P. Stauss, *Spectrochim. Acta Part B At. Spectrosc.*, 1993, **48**, 951–976.
29 B. Welz and M. Melcher, *Anal. Chim. Acta*, 1981, **131**, 17–25.
30 J. Dědina, *Anal. Chem.*, 1982, **54**, 2097–2102.
31 P. Novotný and J. Kratzer, *Spectrochim. Acta - Part B At. Spectrosc.*, 2013, **79**–**80**, 77–81.
32 J. Kratzer, *Spectrochim. Acta - Part B At. Spectrosc.*, 2012, **71**–**72**, 40–47.
33 E. Pagliano, M. Onor, J. Meija, Z. Mester, R. E. Sturgeon and A. D'Ulivo, *Spectrochim. Acta - Part B At. Spectrosc.*, 2011, **66**, 740–747.
34 D. L. Nunes, E. P. Dos Santos, J. S. Barin, S. R. Mortari, V. L. Dressler and É. M. De Moraes Flores, *Spectrochim. Acta - Part B At. Spectrosc.*, 2005, **60**, 731–736.
35 M. Sáenz, L. Fernández, J. Domínguez and J. Alvarado, *Spectrochim. Acta - Part B At. Spectrosc.*, 2012, **71**–**72**, 107–111.
36 W. W. Ding and R. E. Sturgeon, *J. Anal. At. Spectrom.*, 1996, **11**, 421–425.
37 P. Pohl, I. J. Zapata and N. H. Bings, *Anal. Chim. Acta*, 2008, **606**, 9–18.
38 M. H. Arbab-Zavar, M. Chamsaz, A. Yousefi and N. Ashraf, *Talanta*, 2009, **79**, 302–307.
39 E. Nováková, P. Rychlovský, T. Resslerová, J. Hraníček and V. Červený, *Spectrochim. Acta - Part B At. Spectrosc.*, 2016, **117**, 42–48.
40 A. R. Kumar and P. Riyazuddin, *Anal. Sci.*, 2005, **21**, 1401–1410.
41 Y. Gao, M. Xu, R. E. Sturgeon, Z. Mester, Z. Shi, R. Galea, P. Saull and L. Yang, *Anal. Chem.*, 2015, **87**, 4495–4502.
42 O. Linhart, J. Smolejová, V. Červený, J. Hraníček, E. Nováková, T. Resslerová and P. Rychlovský, *Monatshefte für Chemie*, 2016, **147**, 1447–1454.
43 M. Rybínová, S. Musil, V. Červený, M. Vobecký and P. Rychlovský, *Spectrochim. Acta Part B At. Spectrosc.*, 2016, **123**, 134–142.
44 M. Sáenz, L. Fernández, J. Domínguez and J. Alvarado, *Electroanalysis*, 2010, **22**, 2á42-2847.
45 J. Dědina, W. Frech, A. Cedergren, I. Lindberg and E. Lundberg, *J. Anal. At. Spectrom.*, 1987, **2**, 435–439.